

University of Nevada, Reno

**Region-wide patterns and drivers of demographic rates
for a foundation tree species along its dry range margin**

A thesis submitted in partial fulfillment of the requirements for the degree of
Masters of Science in Natural Resources and Environmental Science

by

Jacob A. Macdonald

Dr. J. Hall Cushman/Thesis Advisor

December, 2020



THE GRADUATE SCHOOL

We recommend that the thesis
prepared under our supervision by

JACOB MACDONALD

entitled

**Region-Wide Patterns and Drivers of Demographic Rates for a
Foundation Tree Species Along its Dry Range Margin**

be accepted in partial fulfillment of
the requirements for the degree of

MASTER OF SCIENCE

J. Hall Cushman, Ph.D.
Advisor

Peter Weisberg, Ph.D.
Committee Member

Jonathan Greenberg, Ph.D.
Committee Member

Matthew Forister, Ph.D.
Graduate School Representative

David W. Zeh, Ph.D., Dean
Graduate School

December, 2020

Preamble

The research presented in this thesis is in manuscript form and intended for publication in a peer-reviewed journal. I will be the lead author on the paper, with Tyler Refsland and Hall Cushman as co-authors. Accordingly, I use plural pronouns instead of singular ones throughout the manuscript.

Abstract

Forests are a dominant feature of many terrestrial landscapes throughout the world and have large influences on critical biogeochemical processes and a wide range of other ecosystems services. Unfortunately, many tree species have been reported to be in decline, and increasing temperatures and drought have been implicated as important drivers of this change. To gain a more comprehensive understanding of tree performance during a period of unprecedented anthropogenic climate change, we need to assemble and evaluate demographic data for tree species over longer time periods and across large expanses of their geographic ranges, which often vary substantially in climate and topography. Here, we focus on quaking aspen (*Populus tremuloides*), the most widespread tree species in North America, because it is recognized as a foundational species and has undergone decline in numerous parts of its range. We evaluated the patterns and drivers of recruitment, growth, and mortality of aspen along the more arid parts of its range within a network of 184 aspen-monitoring plots distributed across five states in the western U.S. during a 10–13-year study period. We found that the mortality rate for mature aspen stems was high (mean = 4.3% per year) across all four geographic regions in our study area: Sierra/Cascades, Great Basin, Middle Rockies, and

Wasatch/Colorado Plateau. Consequently, the live basal area of aspen decreased by 2% per year while that of co-occurring conifer species collectively increased by 4.4% per year. We found aspen demographic rates did not vary significantly among the four geographic regions in our study area. Model comparisons revealed that initial stand structure was among the best-performing predictors of aspen performance. Stands composed of fewer, smaller mature stems were associated with faster growth rates, higher sapling density, and increased recruitment into the mature size class (≥ 12.7 cm diameter at breast height). Variables related to summer and annual water balance predicted several aspen response variables, indicating that warmer temperatures and/or drier conditions were associated with faster growth rates, higher sapling and immature aspen densities, and — surprisingly — less mortality. Finally, variables that are either influenced by or correlated with winter and early growing season temperatures were associated with less mortality, increased mature stem recruitment, and higher immature aspen densities. Collectively, our findings indicate that temperature influences demographic rates of all aspen size classes, warranting further research into how interactions among heat, water availability, and evaporative demand, as well as the annual timing of these factors, affect aspen performance. This study documents a decline of aspen populations over the past 10-13 years within its dry range margin that is pervasive across large spatial scales. Despite this result, aspen performance is highly variable at smaller spatial scales, indicating that much of the variation in aspen performance is driven by landscape-scale factors including stand structure, topography, and variations in local climate.

Keywords: Climate change, forest dieback, growth rates, demographic rates, *Populus tremuloides*, recruitment, mortality rates, stand dynamics.

Acknowledgements

I would like to thank my advisor Hall Cushman for his expert mentorship and all the support he has given me. I would also like to thank my lab mate, Tyler Refsland, for his generous contributions of time and effort, and his invaluable input into this project. I am grateful to Danny Cluck and John Guyon for establishing the aspen plot network and providing logistical assistance for our project. Molly Willoughby, Stephen Zipkin and especially Elizabeth Reikowski provided essential assistance with all field work. Tom Dilts contributed invaluable assistance with generating numerous predictor variables. Jonathan Greenberg, Peter Weisberg and Matt Forister provided helpful guidance on this project and commented on the manuscript. J.H.C. is grateful to Kyle Merriam (U. S. Forest Service) for introducing him to the aspen plot network. This project was generously supported by grants from the Nevada Department of Wildlife and USDA's Hatch Program to J.H.C.

Table of Contents

Preamble	i
Abstract	i
Acknowledgments.....	iii
Table of Contents	iv
List of Tables	v
List of Figures	vi
Introduction.....	1
Methods.....	5
Results.....	21
Discussion	26
Literature Cited	37
Figure Legends.....	46
Figures.....	49
Tables	60

List of Tables

Table 1. Climate predictor variables of aspen performance.

Table 2. Topographic predictor variables of aspen performance.

Table 3. Stand structure and composition predictor variables of aspen performance.

Table 4. Best-performing models of aspen performance.

Table S1. Terms included in candidate generalized linear models of aspen performance.

List of Figures

Figure 1. Aspen monitoring plot location map.

Figure 2. Immature aspen stem density bar graphs.

Figure 3. Aspen and conifer change in live basal area bar graph.

Figure 4. Marginal effect plots of aspen mortality rate model terms.

Figure 5. Marginal effect plots of aspen recruitment rate model terms.

Figure 6. Marginal effect plots of aspen growth rate model terms.

Figure 7. Marginal effect plots of aspen sapling density model terms.

Figure 8. Marginal effect plots of aspen juvenile density model terms.

Figure 9. Marginal effect plots of aspen sucker density model terms.

Figure S1. Correlation matrix of aspen response variables.

Figure S2. Correlation matrix of best-performing predictor variables.

1. Introduction

Forests cover 30% of the globe's terrestrial surface area (Keenan et al. 2015) and provide a diverse range of ecosystem services, including the maintenance of biodiversity, hydrological and nutrient cycling, and carbon sequestration (Bonan 2008, Pan et al. 2011, Trumbore et al. 2015). However, there is growing concern that many tree species are in decline due to large-scale tree mortality, contracting stand cover, and/or reduced recruitment (Breshears et al. 2005, van Mantgem et al. 2009, Allen et al. 2010, Peng et al. 2011, Anderegg et al. 2013b, Allen et al. 2015, Millar and Stephenson 2015, Trumbore et al. 2015, Cohen et al. 2016). Increased temperatures and drought associated with anthropogenic climate change are frequently recognized as important drivers of this decline around the world (Allen et al. 2010, 2015). However, it is often unclear 1) how pervasive decline is across large swathes of tree species' ranges and 2) the extent to which climatic and topographic factors — along with stand structure, forest composition, disturbances, and herbivore pressures — mediate tree performance. Thus, understanding the dynamics and spatial extent of tree decline, as well as the many individual and interacting drivers of decline, are of great importance given the essential role that trees play in ecological systems.

Recent reports of large-scale mortality and recruitment failure of quaking aspen (*Populus tremuloides*), the most widely distributed tree species in North America (Perala et al. 1990), indicate that the significant ecosystem services this species provides are under threat. Because aspen's expansive range encompasses a large degree of

environmental heterogeneity, it offers an excellent opportunity to study the effects of climate and topography on tree demographic rates.

Numerous factors have been implicated in the recent demographic decline of aspen, including fire suppression (Shinneman et al. 2013), conifer encroachment (St. Clair et al. 2013), herbivory from insects (Hogg et al. 2002, Chen et al. 2018) as well as wild and domestic ungulates (Beschta and Ripple 2009, Eisenberg et al. 2013, Seager et al. 2013), fungal pathogens (Marchetti et al. 2011, Zegler et al. 2012), and climate change (Worrall et al. 2008, Huang and Anderegg 2012). Although stress-induced mortality and recruitment failure have been reported in several parts of aspen's more arid range in the western U.S. (Kaye et al. 2005, Huang and Anderegg 2012, Zegler et al. 2012) and Canada (Hogg et al. 2002, Michaelian et al. 2011), responses of this influential tree species are known to vary substantially (Yang et al. 2015, Shinneman and McIlroy 2019), and considerable uncertainty remains as to why certain populations are more susceptible to mortality and recruitment failure than others.

Many authors have found that metrics related to water stress, such as climatic water deficit, have been the most successful at predicting aspen dieback and mortality (Rehfeldt et al. 2009, Worrall et al. 2013, Anderegg et al. 2015, Chen et al. 2018). However, studies have found considerable spatial variation in how well climate predicts the growth (Dudley et al. 2015) and dieback (Worrall et al. 2013) of aspen. Studies that examine the effect of climate as well as mediating factors, such as stand structure and topography may help explain these discrepancies.

Topography strongly influences microsite conditions in the montane landscapes that aspen commonly inhabits, and thus should be an important driver of tree performance. However, to date results on this relationship have been variable. For example, studies have shown that topographic features associated with warmer, drier microsities (i.e., solar radiation index or more southerly aspects) can be associated with less mortality, at least among relatively small aspen stems (Bell et al. 2015), or can experience greater mortality (Worrall et al. 2008, Huang and Anderegg 2012). These mixed results may be due to context dependencies in the effect of topography on aspen, as the studies by Worrall et al. (2008) and Huang and Anderegg (2012) were focused on areas that experienced severe drought, while Bell et al. (2015) was not. However, another study, also following severe drought (Kane et al. 2014), failed to detect a relationship between aspen mortality and topography, which highlights the need for additional research that explores the ways that topography interacts with other drivers to affect aspen performance.

While many studies have found that climate is the dominate driver of aspen performance, others have reported that stand structure and composition are more important (Bell et al. 2014, Zhang et al. 2015). Stand age, density, basal area, and structural diversity, as well as stem diameter have been found to affect the mortality rate of aspen (Luo and Chen 2013, 2015, Bell et al. 2014, Zhang et al. 2015, Hember et al. 2017, Trugman et al. 2018, Kweon and Comeau 2019). Similarly, stand stem density and basal area (BA) have been shown to strongly influence aspen growth (Canham et al. 2006, Zhang et al. 2015, Trugman et al. 2018) and recruitment rates (White et al. 2003).

It is unclear what the relative contribution of different drivers are to aspen performance, which drivers are the most significant in different parts of aspen's range, and how interactions among drivers affects aspen performance. Additionally, most studies have focused on growth, dieback, and mortality of mature aspen stems, and it thus remains unclear to what extent the drivers of performance vary among aspen stems of different ages. It is also still unclear how aspen performance varies across its extensive, climatically heterogeneous range. For example, there have been few studies of aspen performance in some parts of its dry range margin, including California, Nevada, and Idaho (but see Bell et al. 2014, Shinneman and McIlroy 2019, McIlroy and Shinneman 2020). These areas are topographically complex, contain forests of diverse ages, structures, and compositions, and have experienced severe drought in the past 20 years. Thus, studies in these areas will be particularly useful at elucidating the relationships among climate, topography, and stand structure in mediating aspen demographic rates.

To address these knowledge gaps, we use an extensive plot network distributed across five states in the western U.S. to address the following questions: 1) To what extent do the densities of immature aspen and the recruitment, growth, and mortality rates of mature aspen vary across different geographic regions in the western U.S. over the past 10–13 years?; 2) Do aspen and co-occurring conifers differ in their performance across this plot network during the same time period?; and 3) What climatic, topographic, and stand structure/composition variables best predict the densities of immature aspen and the recruitment, growth, and mortality rates of mature aspen in the western U.S. over the past 10–13 years?

2. Methods

2.1 Study System

Our study was conducted across an extremely heterogeneous landscape spanning five states: California, Nevada, Idaho, Wyoming, and Utah (Figure 1). The western portion of our study region contained portions of the Sierra Nevada and Cascade mountain ranges. The central portion of the study region was located primarily within the Great Basin, extending north into the Snake River Plain and Idaho Batholith region (hereafter referred to simply as ‘Great Basin’ for brevity). The northeastern portion of our study region contained mountain ranges of the Middle Rocky Mountains, and the southeast portion contained portions of the Wasatch Mountains and Colorado Plateau.

Mean annual precipitation varied greatly across our study region, being wettest in the Sierra Nevada and Cascade mountains (from 368 to 1449 mm per year within our field sites) and driest in the Great Basin (from 264 to 470 mm per year within our field sites). The Sierra Nevada and Cascade portion of the study region experiences a Mediterranean-type climate, receiving almost no precipitation during the summer. The Great Basin receives a slightly larger portion of its precipitation during the summer, while the Middle Rocky Mountains, Wasatch Mountains, and Colorado Plateau receive much more of their precipitation during the summer.

Quaking aspen is a fast-growing, shade-intolerant, deciduous hardwood species. As the most abundant broadleaved tree species in Canadian boreal forests (Peterson and Peterson 1992) and one of the few deciduous tree species in western U.S. forests, aspen

are considered to be a foundation or even keystone species (Rogers et al. 2020). Although aspen can reproduce sexually (Mock et al. 2008), it propagates primarily asexually by suckering from roots, and clones can be very long lived (Kemperman and Barnes 1976). This species commonly regenerates after fire, varies in ploidy level across its range, and exists as both successional stages as well as relatively stable, persistent stands (Shinneman et al. 2013, Callahan et al. 2013). Aspen occurs in relatively high-elevation sites within the study region, with our field plots ranging from 1,273 to 3,155 m in elevation.

In much of the Sierra Nevada and Cascade Mountains, co-occurring conifers included ponderosa pine (*Pinus ponderosa*), Jeffrey pine (*P. jeffreyi*), lodgepole pine (*P. contorta*), incense cedar (*Calocedrus decurrens*), white fir (*Abies concolor*), red fir (*Abies magnifica*), and Douglas fir (*Pseudotsuga menziesii*). In the portion of the Cascades lying near the California–Nevada border, aspen co-occur with red fir and western juniper (*Juniperus occidentalis*). In the Great Basin, aspen co-occur with single leaf pinyon pine (*P. monophylla*), limber pine (*P. flexilis*), and Douglas fir. In the Middle Rocky Mountains, aspen co-occur with subalpine fir (*Abies lasiocarpa*), Douglas fir, limber pine, lodgepole pine, and Utah juniper (*Juniperus osteosperma*). In the Wasatch Mountains and Colorado Plateau, aspen co-occur with Engelmann spruce (*Picea engelmannii*) and subalpine fir.

2.2 Aspen Plot Network

We addressed our research questions with data collected from a network of 184 long-term plots established by the United States Forest Service in aspen stands

throughout California, Idaho, Nevada, Utah, and Wyoming (Figure 1). The network contained 62 plots that were established in 2006 (27 plots in central and northeast Nevada, 31 plots in central and southern Utah, and four plots in western Wyoming); (Guyon and Hoffman 2011), 46 plots that were established in 2007 (all in southern Idaho); (Guyon and Hoffman 2011), and 75 plots that were established in 2009 (in northeastern California); (Cluck 2011). The plot-selection criteria were somewhat different for plots established in California than those established in other states. Specifically, the location of non-Californian plots were randomly chosen from within areas of known recent aspen dieback based on aerial surveys, were within one mile of a road, and contained at least seven overstory aspen stems within the plot borders (Guyon and Hoffman 2011). In contrast, plot locations in California were chosen from within areas of previously mapped aspen cover (but not necessarily areas of dieback), were in close proximity to roads, and contained at least two live mature aspen stems within the plot (Cluck 2011). Aspen stands in California were typically small and plot selection was biased toward larger stands to ensure that they contained the minimum required number of live mature aspen stems (Cluck 2011). Seven of the 75 plots in California were chosen from within aspen stands that had recently received conifer-removal treatments.

All plots were circular in design, with an 8.02 m radius and contained three 2.07 m radius subplots. Plot centers were monumented with a metal U post, and all trees with ≥ 12.7 cm diameter at breast height (DBH) were permanently marked with metal tags.

2.3 Field Sampling

All 184 plots were initially sampled between in 2006, 2007 or 2009 (see above) and then again between June and September of 2019 to assess mortality, growth, and recruitment rates of mature aspen stems, as well as the density of immature aspen stems and percent cover of understory vegetation. During the first and second samplings, the DBH, species, canopy dieback rating, and status (alive/dead) were recorded for all mature trees (defined as $DBH \geq 12.7$ cm) in each plot. Canopy dieback was quantified into four categories: no dead branches in crown; 1–33% of branches in crown dead; 34–66% of branches in crown dead; and 67–100% of branches in crown dead.

During the first and second sampling, regeneration was quantified by counting all aspen stems with $DBH < 5.1$ cm within each of the three subplots. In order to study regeneration of different size classes, we counted seedlings/suckers ($DBH < 5.1$ cm and less than 1 m tall) and juveniles ($DBH < 5.1$ cm and more than 1 m tall) separately during the second plot sampling. Although true seedlings may exist, we refer to aspen seedlings/suckers simply as suckers throughout the text.

Additionally, during second sampling, we counted seedlings and juveniles of all non-aspen tree species, and visually estimated the percent cover of herbaceous species and non-aspen woody species in the understory for each subplot. We recorded percent cover as the percent of the subplot's surface area covered by the vertical projection onto the ground of plants in the understory such that both herbaceous and woody cover estimates could be up to 100% simultaneously. Percent covers were estimated into 11 cover classes (0%, > 0–10%, 11–20%, 21–30% ...). Non-aspen tree seedlings and

juveniles were included in estimates of woody cover, but trees with a DBH ≥ 5.1 cm were excluded from estimates.

We recorded the presence of any streams within the plot boundaries that contained running water at the time of the second sampling. We also recorded slope and aspect, as well as the number of cut down conifer stumps within the plot boundary. We measured the plot center location to within 3 m accuracy with an Eos Arrow 100 GPS unit.

2.4 Soil Analyses

In order to assess how aspen performance varied with soil organic carbon (C) and total nitrogen (N), we collected soil samples from each plot during the second sampling. We collected a single soil core to a depth of 16.2 cm, located within 2 m of the plot center. Soil samples were sealed in zip-lock bags until we returned from the field (between 1 and 25 days), then allowed to air dry and stored for approximately 6 months at room temperature before analysis. Soil samples were processed and analyzed by the Soil, Water and Forage Analytical Laboratory at Oklahoma State University. Percent mass of soil organic C and total N were determined using a dry combustion C/N analyzer (Leco CN628, LECO Corp, St Joseph, Michigan, USA); (Nelson and Sommers 2018).

2.5 Response Variables

We used data from our field sampling to calculate six plot-level response variables: annual percent mortality, annual percent recruitment of mature stems, growth rate, sapling density, juvenile density, and sucker density.

Annual percent mortality was calculated as the percent of mature aspen stems that died between the two sampling periods, normalized by the number of years between samplings (Equation 1).

$$\text{Equation 1. Annual percent mortality} = \frac{(n_I - n_F)/n_I}{Y_F - Y_I} (100\%)$$

Here n_I equals the number of live mature aspen stems present in a plot in the initial sampling, n_F equals the number of mature aspen stems present and alive in both samplings, and Y_I and Y_F equal the years of initial and final samplings, respectively.

Annual percent recruitment of mature stems was the number of live aspen stems in each plot that transitioned into the mature stem size class during the study period, normalized by the number of years between sampling dates and by the number of mature aspen stems in the plot during the initial sampling, to account for differences in duration of the study period, and differences in overall clone stem densities (Equation 2).

$$\text{Equation 2. Annual percent recruitment of mature stems} = \frac{n_R/n_I}{Y_F - Y_I} (100\%)$$

Here n_R equals the number of aspen that recruited into the mature aspen size class during the study period.

The metric we chose to use for growth rate was the percent change in individual basal area (BA), divided by the number of years between samplings, averaged across all surviving mature aspen stems in each plot (Equation 3).

$$\text{Equation 3. Growth rate} = \frac{\left(\sum_{i=1}^{n_F} \frac{BA_{Fi} - BA_{Ii}}{BA_{Ii}} \right) / n_F}{Y_F - Y_I} (100\%)$$

For each individual mature aspen stem, i , BA_{Ii} and BA_{Fi} equal their BA during the initial and final samplings, respectively.

Because saplings, juveniles, and suckers were not permanently tagged, we were unable to calculate growth, mortality, or recruitment rates for them. Instead, we used density of live stems in the final sampling as a response variable for each of these size classes.

2.6 Predictor Variables of Aspen Performance

2.6.1 Climate variables

Based on previous studies of climate-driven patterns in aspen demographic rates, we selected seven climate variables to summarize from monthly climate data (Table 1a). We used data available from TerraClimate (Abatzoglou et al. 2018), which provides interpolated monthly climate data at 4-km resolution. The climate variables of interest were precipitation accumulation, daily high temperature, vapor pressure, vapor pressure deficit (VPD), climatic water deficit (CWD), snow water equivalent (SWE), and Palmer drought severity index (PDSI). We generated several summaries, each of which was calculated over two different time periods. The first time period was the duration between plot establishment and resampling (i.e., 2006, 2007, or 2009 — depending on plot — through 2019), and climate variables summarized over this timer period were used to model all of our aspen response variables except mortality rate. The second time period

was the interval beginning five years prior to plot establishment and ending upon plot resampling (i.e. 2001, 2002, or 2004 — depending on plot — through 2019). Climate variables summarized over this second time period were used to model aspen mortality rate. This extended time period was chosen to account for the possibility that mortality may have a lagged relationship with climate (Rogers et al. 2018). We calculated the following summaries, averaged over each of the two time periods, for each climate variable (see Table 1a for climate summary definitions): 1) mean annual value/mean seasonal value for winter (Dec–Feb), spring (Mar–May), summer (Jun–Jul), and fall (Sep–Nov); 2) mean annual difference from normal; and 3) annual deviation/seasonal deviation for winter, spring, summer, and fall. Additionally, we included the maximum value of summer temperature and minimum value for annual and seasonal Palmer drought severity index because single extreme heat or drought events may cause mortality even if average climate conditions over the study period are within aspen’s tolerance.

To account for large climatic differences across our study area, we also included climate normals, available from WorldClim version 2 (Hijmans et al. 2005), which provides interpolated 30-year averaged (1970–2000) climate variables at 1-km resolution. Many of the variables provided by WorldClim are highly correlated with our summaries from monthly data (e.g., WorldClim’s ‘precipitation of the wettest quarter’ is equivalent to our mean winter precipitation). However, we included five variables from WorldClim that provided information not present in our summaries from TerraClimate. These

variables were diurnal temperature range, annual temperature range, temperature isothermality, temperature seasonality, and precipitation seasonality (Table 1b).

2.6.2 Topographic variables

We calculated several variables to assess the role that topography plays in mediating the effect of climate and how microsite conditions influence aspen performance. Details for all topographic variable derivations can be found in Table 2. We derived the following variables from data collected in the field: stream presence (a categorical predictor), elevation, slope, folded aspect (rescaling aspect values between 180° and 360° to range from 0 to 180° , such that $NE = NW = 45^\circ$, $E = W = 90^\circ$, etc.), potential solar radiation, and heat-load index. We also calculated several variables in arcMap using USGS digital elevation models. We calculated topographic-wetness index (a proxy for cold air drainage and soil moisture), topographic-position index (a location's elevation relative to the average elevation of the surrounding neighborhood), curvature (the degree of concavity or convexity of a slope), profile curvature (curvature parallel to the direction of maximum slope), and planform curvature (curvature perpendicular to the direction of maximum slope).

2.6.3 Stand structure and composition variables

Because stand age, stem density, and individual differences in tree size and morphology all likely influence aspen performance, we calculated several variables relating to stand structure and composition from our field data (Table 3). We calculated the following metrics for mature trees in the initial sampling: BA, tree count, mean BA of

individual trees, standard deviation of individual BA, and quadratic mean diameter. Each of these metrics were calculated for several different subsets of the stand (e.g., live aspen only, live conifers only; see Table 3 for complete list). We also included the sum of aspen suckers and juveniles in the initial sampling as a predictor, primarily to help accurately model sapling density in the final sampling. However, ‘initial suckers plus juveniles’ was excluded as a predictor when modeling sucker density and juvenile density; no distinction was made between suckers and juveniles during the initial sampling, and it would not be reasonable to model a single one of these size classes as a function of both size classes pooled together. The number of non-aspen seedlings plus juveniles in the final sampling was also used as a predictor variable, primarily to characterize the competitive environment of the smaller aspen size classes. Finally, we quantified the relative abundance of aspen in the initial sampling in two ways: the ratio of aspen trees to the total number of trees, and the ratio of live aspen BA to the total live BA.

2.6.4 Biological, geographic, and soil variables

We included several other variables that we hypothesized would influence aspen performance. We included mean canopy dieback rating of all live mature aspen stems in each plot in the initial sampling (the minimum value of zero would indicate no dieback in any aspen, and the maximum value of 3 would indicate between 67 and 100% dieback in all aspen), in order to account for differences in stand health at the onset of the study, and to mitigate for possible biases due to differing plot-selection criteria in California compared to the other states. We included state, region, latitude, and longitude to assess larger-scale geographic patterns in aspen performance. We also included the following

non-aspen variables: growth rate of conifers (calculated the same as for the aspen response variable, shown above); percent cover of woody species and of herbaceous species, primarily to characterize the competitive environment for suckers and juveniles; number of conifers removed; duration in years between plot samplings; and percent nitrogen, carbon, and total organic matter, of the soil. Finally, when modeling sucker density and juvenile density only, we included aspen mortality rate and aspen growth rate as predictor variables in order to assess whether the health and vigor of the mature aspen in a stand influenced suckering and survival of suckers and juveniles.

2.7 Data analyses

2.7.1 Geographic pattern analyses

We evaluated the degree to which each of our response variables varied across four broad geographic regions: Sierra/Cascades, Great Basin, Middle Rockies, and Wasatch/Colorado Plateau. These regions were chosen based on geographic clustering of plots and distinguishing environmental conditions. Specifically, the Sierra/Cascades experience a Mediterranean climate, setting them apart from the other study regions. The Great Basin plots were distinguished by occurring in relatively wet, high-elevation sites among an otherwise extremely arid landscape. The Wasatch/Colorado Plateau region has documented occurrences of sudden aspen decline — a primarily climate-driven phenomenon (Worrall et al. 2010) — unlike the other study regions. The Middle Rockies receive more annual precipitation than either the Wasatch/Colorado Plateau or Great Basin regions, and receive significant amounts of precipitation in the summer, unlike the Sierra/Cascades.

We tested the hypothesis that our aspen response variables varied across the four regions using permutation ANOVA tests. All permutation tests were run with 10,000 permutations using the RVAideMemoire package version 0.9-77 (Hervé 2020) in R version 3.6.3 (R Core Team 2020). For response variables that varied significantly among regions, we followed up with permutation t-tests to evaluate differences among means ($\alpha = 0.05$). We adjusted t-test p values for multiple comparisons using the Benjamini and Hochberg (1995) method.

2.7.2 Correlations among response variables

To determine whether our various aspen response variables covaried with each other, we calculated pairwise correlation coefficients between each response variable. We used Kendall's τ_b to test the associations between variables because it allowed us to test for monotonic, but not necessarily linear, relationships.

2.7.3 Correlations among predictor variables

We calculated pairwise Pearson correlation coefficients between all predictor variables present in our best-performing models, as well a select few additional predictor variables (mean high temperature for winter, spring, summer, and fall, and mean individual aspen BA) in order to aid us in the qualitative interpretation of our results. Because many of the predictor variables were highly correlated, this information allowed us to better understand the commonalities between the best-performing model for each aspen response variable, despite the multiplicity of variables contained in them. A matrix of Pearson correlation coefficients between predictor variables is shown in Figure S2.

2.7.4 Comparison between aspen and conifer performance

To compare the demographic trends of aspen and co-occurring conifers across the different regions, we calculated the plot-level annual percent change in live BA of mature tree stems over the study period, as this metric allowed us to compare the combined effects of mortality, adult recruitment, and growth in a single analysis. We used a permutation two-way ANOVA to evaluate the effects of taxonomy (aspen versus conifer), region (Sierra/Cascade, Middle Rockies, and Wasatch/Colorado Plateau), and their interaction on annual percent change in BA, followed by pairwise permutation t-tests for response variables that varied significantly among regions. The tests were carried out using the same methods as those described above for the geographic pattern analyses. Given the comparison of trends among aspen and co-occurring conifers required that plots contained at least one mature conifer in the initial sampling, this analysis was restricted to a subset ($n = 85$) of the total number of plots ($n = 184$), none of which were in the Great Basin region.

2.7.5 Modeling aspen performance — Overview

We used a two-step process to determine which climate, topographic, and stand structure/composition variables best predicted aspen performance. First, we used random forest regressions to select the 15 most important predictor variables for each response variable from the large set of potential predictors. Second, we created candidate generalized linear models for each response using the list of 15 predictors and assessed their performance using AIC. The approach of using random forest to select variables of high explanatory power, for subsequent use in generalized linear models or other

modeling techniques has been used successfully in the past with ecological datasets (Arthur et al. 2010, Seidl et al. 2011), and allowed us to assess a much larger set of predictors than would be computationally practical with AIC based model selection techniques alone.

2.7.6 Modeling aspen performance — Variable reduction

To select the set of 15 predictors for each response, we employed a stepwise elimination process. We began by running a random forest regression with the full set of potential predictors ($n = 144$ for mortality, growth, mature stem recruitment, and sapling density; $n = 145$ for sucker and juvenile densities), then removing the predictor with the lowest variable importance score (as measured by percent increase in mean squared error). We then repeated this procedure with the new set of predictors until only 15 variables remained. The analysis was carried out using the RandomForest package version 4.6-14 (Liaw and Wiener 2002) in R. All random forest models were created with 500 trees and $n/3$ variables tried at each node, where n is the number of variables in each regression.

2.7.7 Modeling aspen performance — Generalized linear modeling

We arrived at a final model for each response variable by selecting from all candidate models the one with the lowest AIC. For each response, the fully-saturated model contained the 15 predictors resulting from the stepwise selection process, as well as 3 to 5 interaction terms (Table S1). Predictors were centered to avoid inflation of coefficient estimate standard errors, and to allow for meaningful interpretation of main

effect coefficients in the presence of interaction terms (Schielzeth 2010). Because we were interested in how the effects of environmental conditions (i.e. climate or topography) on aspen performance are mediated by intrinsic stand characteristics, we chose interaction terms that fit into the categories of climate x stand structure/composition, and topography x stand structure/composition. We also included climate x topography interactions in order to classify microsite conditions experienced by the stand, which may differ from the relatively coarse scale climate data. Decisions about which predictors to include in these interaction categories were guided by the performance of variables in preliminary analyses with no interaction terms, and by variable combinations we believed to be biologically relevant, a priori.

We used the package MuMIn version 1.43.15 (Barton 2019) in R to rank generalized linear models for each response based on AIC or AIC_C (see below). Candidate models included all possible models nested within the saturated model, that met the following criteria: the maximum number of terms was nine; pairs of predictors with a Pearson correlation coefficient of 0.65 or greater were excluded from appearing in the same model; and the variance inflation factor (VIF) for all terms in the model was less than two. The highest ranked model was then checked for highly influential points. If any were present, the points were removed and candidate models refitted and reranked. Following this procedure, the highest ranked model was assessed for meeting the assumptions of linear regression and possible model misspecifications, using the diagnostic tools in the DHARMA package version 0.3.1 (Hartig 2020) in R. We checked that the distribution of standardized residuals was approximately uniform with respect to

residual rank and with respect to each predictor in the model. We also used DHARMA's tests for over/under dispersion and zero inflation. If the highest ranked model did not meet these criteria, the highest-ranked model that did meet these criteria was chosen as our final model.

Annual percent mortality was modeled using a Gaussian error distribution and an identity link function, as was growth rate after being log transformed. These two models were ranked based on AIC_C . Annual percent recruitment of mature stems as well as sapling, juvenile, and seedling density were all modeled with a negative binomial error distribution and a log link function. These models were ranked by AIC rather than AIC_C because AIC_C has been shown to be ineffective at reducing biases of relative, expected Kullback-Liebler divergence estimates when used for models with non-Gaussian error distributions (Richards 2005). Because mature stem recruitment was modeled with a negative binomial model, the response variable used for the purpose of linear modeling was simply the number of aspen stems that transitioned into the mature stem size class during the study period. This number was then normalized by using an offset equal to the number of years between samplings multiplied by the number of live mature aspen stems in the initial sampling, to account for differences in duration of the study period, and differences in overall clone stem densities. Similarly, the actual response variable used in the negative binomial models for saplings, juveniles, and suckers, was the stem count in each plot. However, because our plots were all equal in area, density and count are equivalent. Predicted values generated from our models were transformed to densities so

that they could be compared directly to values reported in other studies, and we refer to density rather than count throughout the text for the sake of consistency.

3. Results

3.1 Geographic Patterns

Aspen mortality, mature stem recruitment, and growth rates did not vary significantly among the four geographical regions that we designated for this analysis ($F_{3,180} = 0.35$, $p = 0.786$; $F_{3,180} = 0.26$, $p = 0.866$; and $F_{3,152} = 0.77$, $p = 0.522$, respectively). The average rate per year across all plots was 4.25% for mortality, 1.22% for mature stem recruitment, and 2.43% for growth.

The overall mean sapling density in 2019 was 0.059 stems m^{-2} and varied significantly among regions ($F_{3,180} = 2.77$, $p = 0.043$; Figure 2a). The Great Basin had the highest density at 0.09 stems m^{-2} and differed from the Middle Rockies, which had the lowest density at 0.04 stems m^{-2} . The regions with intermediate sapling density — the Sierra/Cascades and the Wasatch/Colorado Plateau — did not differ significantly from any other region. The overall mean juvenile density was 0.228 stems m^{-2} and, in contrast with sapling density, did not differ significantly among regions ($F_{3,143} = 1.90$, $p = 0.131$; Figure 2b).

The overall mean sucker density was 0.28 stems m^{-2} and varied significantly by region ($F_{3,143} = 8.22$, $p < 0.001$; Figure 2c). The Sierra/Cascades region had the greatest density at 0.586 stems m^{-2} , followed by the Great Basin region at 0.36 stems m^{-2} , the Wasatch/Colorado Plateau region at 0.16 stems m^{-2} , and the Middle Rockies region at

0.04 stems m^{-2} . The Sierra/Cascades, Wasatch/Colorado Plateau, and Middle Rockies regions all differed significantly from each other. The Great Basin region also differed from the Middle Rockies but not from any other regions.

3.2 Correlations Among Response Variables

There were positive relationships of moderate strength between aspen sucker and juvenile density ($\tau_b = 0.36$; $p < 0.001$), juvenile and sapling density ($\tau_b = 0.31$; $p < 0.001$), sapling density and mature stem recruitment ($\tau_b = 0.26$; $p < 0.001$), and mature stem growth rate and recruitment ($\tau_b = 0.26$; $p < 0.001$; Figure S1). We also found weak positive relationships between mature stem growth rate and sapling density ($\tau_b = 0.19$; $p < 0.001$), and between mortality rate and juvenile density ($\tau_b = 0.18$; $p = 0.002$). There was a weak negative relationship between mature stem growth rate and sucker density ($\tau_b = -0.15$; $p = 0.019$). We found no other monotonic associations between response variables at an $\alpha = 0.05$ significance level.

3.3 Comparison of Aspen and Conifer Performance

We found the annual percent change in live BA was significantly different for aspen and conifers among the six geographic regions (taxonomy x region: $F_{2,164} = 4.08$, $p = 0.021$; Figure 3). Specifically, mean live BA of aspen decreased by 1.98% per year and did not differ by region. In contrast, live BA of conifers increased 4.44% per year, on average, and differed from aspen in all regions. Conifer BA increased most rapidly in the Middle Rockies region at 8.40% per year, which differed significantly only from the Sierra/Cascades, where conifer BA increased at 2.73% per year.

3.4 Modeling Aspen Performance

3.4.1 Variable reduction and interaction terms

The 15 variables selected by the random forest stepwise selection processes for each response variable, as well as the interaction terms we chose to include in candidate linear models, are listed in Table S1.

3.4.2 Mortality rate

The best-performing model predicting annual percent mortality included initial aspen dieback and terms related to climate, topography, and stand structure ($R^2 = 0.39$; Table 4a). The strongest predictor of aspen mortality rate was the initial mean canopy dieback rating of aspen, such that plots with high levels of initial aspen canopy dieback had subsequently high rates of mortality (Figure 4a). Similarly, there was a positive relationship between mortality rate and total standing dead BA in the initial sampling (Figure 4d). In terms of climate, mortality was positively correlated with 30-year normal annual temperature range (Figure 4c), such that mortality rates were greater in plots with larger variation in annual temperature. Mortality was negatively correlated with deviation in annual VPD (Figure 4b), potential incident solar radiation (Figure 4e), and deviation in annual precipitation (Figure 4f). Specifically, aspen mortality rates were lower in plots situated on sunnier slopes that experienced higher-than-normal evaporative demand and higher-than-normal precipitation.

3.4.3 Mature stem recruitment

The best-performing model predicting mature stem recruitment contained terms related to stand structure and climate (McFadden's pseudo $R^2 = 0.103$; Table 4b).

Recruitment was negatively associated with initial aspen live BA (Figure 5a) and mean spring SWE of the study period (Figure 5b). Recruitment tended to be higher in stands with less drought, as measured by mean annual PDSI over the study period (Figure 5c).

3.4.4 Growth rate

The best-performing model predicting log-transformed growth rate contained terms related to stand structure, climate, and topography ($R^2 = 0.265$; Table 4c). Growth rate was most strongly associated with initial total live BA, with faster growth rates in stands with lower BA (Figure 6a). Growth rate was positively associated with mean summer vapor pressure of the study period (Figure 6b) and mean annual high temperature of the study period (Figure 6c), both of which indicate that aspen tended to grow faster in warmer conditions. Growth rate was also positively correlated with the standard deviation of the individual BAs of live aspen in the initial sampling, meaning that plots with greater variation in aspen stem diameter had faster growth rates (Figure 6d). Finally, growth rate was negatively associated with topographic position index, such that aspen located in relatively upland environments had faster growth rates (Figure 6e).

3.4.5 Sapling density

The best-performing model predicting sapling density contained terms related to stand structure, climate, and their interaction (McFadden's pseudo $R^2 = 0.276$; Table 4d). Sapling density was positively associated with the number of aspen suckers plus juveniles

in the initial sampling (Figure 7a), as well as summer water deficits, as indicated by CWD (Figure 7b). Sapling density was negatively associated with both live mature stem BA (Figure 7b) and the total number of live mature trees in the initial sampling (Figure 7c). However, sapling density had a positive association with the interaction term between live BA and mean summer CWD, such that the effect of CWD on sapling density was mitigated for plots with lower BA. For plots with moderately low BA (approximately one standard deviation below the mean), there was no relationship between summer CWD and sapling density at all (Figure 7b).

3.4.6 Juvenile density

The best-performing model predicting juvenile density contained terms related to topography and climate (McFadden's pseudo $R^2 = 0.075$; Table 4e). Juvenile density was positively associated with elevation (Figure 8a), deviation in summer CWD (i.e. plots with greater-than-normal summer water deficits had more juveniles; Figure 8b), and deviation in winter high temperature (Figure 8c).

3.4.7 Sucker density

The best-performing model predicting sucker density contained terms related to topography and climate (McFadden's pseudo $R^2 = 0.330$; Table 4f). Sucker density was most strongly influenced by the presence of a stream, with higher densities found in plots containing a stream (Figure 9a and 9b). Sucker density was positively associated with mean winter VPD, meaning that plots that experienced higher winter evaporative demand had more suckers (Figure 9a). Finally, sucker density was positively associated with

seasonality of precipitation, such that plots with larger seasonal variation in precipitation had higher sucker density (Figure 9b).

4. Discussion

We leveraged a large network of forest inventory plots established within aspen stands and distributed across five states in the western U.S. to examine patterns and drivers of aspen performance during a 10–13-year period. Our study provides important insights into the context-dependency of aspen performance across topographically heterogeneous, semi-arid environments that represent the more arid margin of aspen's geographic range.

We observed high rates of mature aspen mortality ($4.3\% \text{ yr}^{-1}$), with approximately half of all mature aspen stems in our plots dying during the 10–13-year study period. Paired with the lack of correlation between mortality and mature stem recruitment (Kedall's $\tau_b = -0.08$) and low recruitment rates overall ($1.2\% \text{ yr}^{-1}$), our findings indicate that the majority of the aspen stands in our study are failing to regenerate, either due to successional processes or stress-induced decline. Although aspen demographic rates did not vary substantially among geographic regions, they were highly variable within regions, even among neighboring plots. The high degree of spatial heterogeneity within geographic regions highlights that aspen demographic performance is highly contingent on landscape and stand-level processes.

We found that mortality strongly increased with the severity of initial canopy dieback and decreasing evaporative demands (as measured by deviation in annual VPD), whereas mature stem recruitment and growth were greatest in stands with lower initial

BA. Similarly, the density of saplings was greatest in stands with fewer, smaller mature trees that experienced high summer CWD during the study period. The performance of smaller aspen size classes was primarily associated with climate and topography. Juvenile density was greatest at high elevation sites that have recently experienced drier than normal summers, and sucker density was greater at sites near streams with high mean winter VPD.

4.1 Effect of initial canopy dieback and standing dead BA

Our best-performing model of aspen mortality showed that stands with higher initial levels of canopy dieback subsequently had higher mortality rates (Figure 4a). A similar association was noted by Zegler et al. (2012), who found that canopy dieback was correlated with percent dead aspen BA. Our findings were also consistent with those of Anderegg et al. (2013c), who found that water-stress-induced embolism of branches and roots, which often results in canopy dieback, predicted the probability of aspen survival. Our results also demonstrate the lagged response of aspen mortality to environmental stress, documented by other authors (Kane et al. 2014, Rogers et al. 2018). Our best-performing mortality model also revealed that stands with greater standing dead BA in the initial sampling had higher subsequent mortality rates (Figure 4d). This finding suggests that stands that experienced elevated mortality in the past tend to deteriorate further with time, similar to the findings of Worrall et al. (2015).

4.2 Effect of stand structure

We found that variables related to initial stand structure were among the best predictors of aspen demographic performance. Specifically, recruitment and growth rates of mature aspen stems were greater in stands with initially low aspen and total BA, respectively (Figures 5a and 6a). Given that aspen is highly shade intolerant (Perala et al. 1990), its growth and recruitment may have been light limited in stands with relatively high BA, consistent with the large number of studies in the western US that have found a negative relationship between competitor density and rates of aspen growth (Brown et al. 2006, Pierce and Taylor 2010, Berrill and Dagley 2012, Bretfeld et al. 2016) and recruitment (Miller et al. 2000, White et al. 2003, Jones et al. 2005, Krasnow and Stephens 2015, Hansen 2016). Furthermore, stands with initially low BA may have been composed of younger, and therefore faster-growing aspen stems, as previously found for the species in the Sierra Nevada (Pierce and Taylor 2010, Berrill and Dagley 2012). Indeed, for our study plots, the initial mean BA of individual aspen stems was positively correlated with initial total live BA ($r = 0.53$; Figure S2).

Additionally, we found aspen growth rate was higher in stands with greater variability in initial individual aspen BA (Figure 6d), suggesting that after accounting for the effect of overall competition (i.e. initial total live BA) in our models, structurally-complex aspen stands (i.e. multi-cohort, uneven-aged stands) achieved higher growth rates than more structurally-uniform stands. Structural-complexity of aspen stands may be indicative of overall clone health and vigor, as suggested by other studies that found that structurally-complex stands had greater survival rates than structurally-uniform stands during mortality events (Worrall et al. 2010).

The density of aspen saplings was negatively associated with both initial total live BA (Figure 7b) and total stem density (Figure 7c). This pattern could be explained by a cohort of aspen establishing, following a past disturbance (Perala et al. 1990, Kashian et al. 2007), or by increased growth and survival of young aspen due to increased light and resource availability in sparser stands. Consistent with both these interpretations, Pierce and Taylor (2010) found that the recruitment of aspen stems into the sapling size class was positively correlated with light availability.

4.3 Effect of summer and annual water balance

Summer and annual water balance variables as well as variables that were strongly correlated with these variables (i.e., mean summer CWD, deviation in summer CWD, deviation in annual VPD, and mean annual high temperature), were important predictors for several of the aspen response variables. Warmer temperatures and/or drier conditions were associated with less mortality, faster growth rate, and higher sapling and juvenile densities.

Contrary to expectations, we found a negative relationship between aspen mortality and deviation in annual VPD, such that stands that experienced higher-than-normal evaporative demands during the study period, had less mortality (Figure 4b). Our results contrast with numerous past studies that have found a positive relationship between aspen mortality and hotter, drier conditions (Hanna and Kulakowski 2012, Bell et al. 2014, 2015, Kane et al. 2014). We speculate that there are at least two potential reasons for the disagreement between our findings and past literature. First, it is possible that VPD deviation was simply acting as a proxy for some other factor driving aspen

mortality. Second, it could be that the temperature component of annual VPD deviation was responsible for decreasing aspen mortality. Although there is strong evidence that extreme heat events may cause mortality in aspen (Rehfeldt et al. 2009, Michaelian et al. 2011, Anderegg et al. 2013a), our VPD deviation variable may not reflect whether or not such events occurred, because it is averaged over such a long time period (15 to 18 years, depending on the plot). A study in the Greater Yellowstone Ecosystem found that aspen cover was lost in areas with fewer growing degree days (Brown et al. 2006). Our VPD deviation variable may be picking up on a similar climate signal of increased growing season length. Aspen photosynthesize through their bark before leaf-out (Foote and Schaedle 1978) and may be able to increase carbon stores in the early growing season, particularly if the period is unusually warm. This could increase survivorship, as carbon starvation is one of the main mechanisms by which drought kills trees (McDowell et al. 2011). Or similarly, VPD deviation may be indicating warmer temperatures during more mesic parts of the year which may enhance carbon assimilation.

In terms of growth of mature aspen, we found a positive relationship between growth rate and mean annual temperature (Figure 6c). In our study region, mean annual temperature was strongly and inversely correlated with elevation, and therefore length of the growing season, which likely contributes to the relationship between temperature and growth. Past studies have found mixed results with regards to the relationship between aspen growth and temperature. Brown et al. (2006) found that aspen radial growth rate increased both with mean annual daily minimum temperature and growing degree days, similar to our own results. Hanna and Kulakowski (2012) on the other hand, found that

aspen growth was negatively correlated with temperature, except at their highest elevation sites, where growth was positively correlated with temperature.

With regard to the performance of immature aspen, juvenile density was positively associated with elevation (Figure 8a) and deviation in summer CWD (Figure 8b), suggesting high-elevation sites that experienced warmer and/or drier conditions than normal during the study period tended to have more juveniles. Similarly, sapling densities tended to be higher in warmer and/or drier sites, as measured by mean summer CWD (which was correlated with summer CWD deviation in our plots; $r = 0.64$; Figure S2). If the survivorship of juveniles, saplings, and mature aspen all respond similarly to environmental conditions, then the same mechanism responsible for the mortality–VPD deviation relationship discussed above (whether it truly is driven by temperature or water balance or an unknown correlated factor) may be responsible for the immature aspen density–water balance relationships as well, via increased survivorship of the smaller size classes. Furthermore, the strength of the effect of summer CWD on sapling density diminishes as stand BA decreases (Figure 7b). This result is consistent with the idea that moderately elevated temperatures increase aspen survivorship via enhanced carbon acquisition; it suggests that in plots with high competition the summer CWD–sapling density relationship is important, but in low competition plots, where carbon acquisition is already easy, the relationship disappears. Previous studies have found mixed results with regards to relationships between temperature and immature aspen performance. Studies that assessed climate variables have found seedling and/or vegetatively produced immature aspen stem densities to increase with temperature (Shinneman and McIlroy

2019), decrease with temperature (McIlroy and Shinneman 2020), or did not find strong relationships with temperature at all (Clement et al. 2019). Hansen et al. (2016) found aspen seedling presence in post-fire sites in Yellowstone to be more likely in warmer sites 11 years post-fire, but less likely in warmer sites 24 years post-fire. Furthermore, they found that of the sites that still contained aspen 24 years post-fire, densities were higher in warmer sites. Studies that have examined the effect of microsite conditions (i.e. elevation and/or south facing aspect) have found that densities are higher in warmer microsities (Turner et al. 2003), or that the direction of the relationship differs for different size classes of immature aspen (Rhodes et al. 2017), or that survivorship of immature aspen is lower in warmer microsities (Zegler et al. 2012). A possible explanation for these mixed results is that extremely high temperatures cause reduced growth or mortality of young aspen, but moderate temperature increase — perhaps at particular parts of the year or when other conditions are met — may be enhancing their performance. Studies such as our own, that lack any intra or inter-annual sampling of aspen performance, do not have the ability to parse out the potentially complex, non-monotonic, and context dependent relationships between aspen performance and temperature with any conclusiveness.

4.4 Effect of winter temperature

Winter temperature variables as well as variables that were strongly correlated with these winter temperature variables (i.e. deviation in winter high temperature, annual temperature range, mean winter VPD, mean spring SWE, and seasonality of precipitation) were important predictors for several aspen response variables. Warmer

winters were associated with less mortality, increased recruitment, and higher juvenile and sucker densities.

Mortality of mature aspen was associated with annual temperature range (which was, itself, correlated with deviation in winter temperature; $r = -0.71$; Figure S2), such that plots with warmer winters had less mortality (Figure 4c). As discussed previously, conditions more conducive to carbon acquisition in the early growing season may have contributed to this pattern.

Similarly, the relationships between juvenile and sucker densities and warmer winters may be due to a lack of mortality in these smaller size classes, driven by the same mechanism. The effect may be particularly pronounced for suckers (which we defined as less than one meter tall) which would not be able to photosynthesis at all when buried under snow. In our sucker model, there are two winter temperature related terms, mean winter VPD and seasonality of precipitation (a variable strongly correlated with deviation in winter temperature; $r = 0.91$; Figure S2), which together account for a larger portion of the variance explained by the model, than did the winter temperature related terms in our best models for the other response variables. This relationship may not hold for aspen stands in elk winter range, however, as snowpack has been found to protect suckers from herbivory (Martin and Maron 2012, Brodie et al. 2012, Rhodes et al. 2017). It is also important to note that there is a strong geographic pattern to some of the winter temperature related variables. The Sierra/Cascade plots, which have a Mediterranean climate, stood out from the rest of the plot network in terms of their annual temperature range, precipitation seasonality, and deviation in winter temperature. We must consider

the possibility that the relationships we found are just a proxy for some other regional differences among plots. However, Shinneman and McIlroy (2019) found a similar relationship between aspen establishment density and winter temperature (five year averaged winter low temperature, centered five years prior to establishment year) in a large study area within the Great Basin.

Finally, mature stem recruitment rates were negatively associated with lower mean spring SWE. Mean spring SWE was not as strongly correlated with the other variables in this group as they were to each other, but this relationship still suggests that warmer early growing season temperatures enhance growth and/or survivorship, leading to more recruitment.

4.5 Effect of drought

Metrics of drought, specifically mean annual PDSI and deviation in annual precipitation, were associated with increased mortality and decreased mature stem recruitment rate, although the effect size was small relative to all other terms our models (Table 4a and 4c). Previous studies have fairly consistently found that wetter conditions are associated with reduced mortality (Hanna and Kulakowski 2012, Anderegg et al. 2013a, Bell et al. 2014, 2015, Kane et al. 2014), faster growth rates (Brown et al. 2006, Chen et al. 2017), higher densities of immature aspen (Rhodes et al. 2017, Clement et al. 2019, McIlroy and Shinneman 2020), and higher proportions of establishment within stands (Kaye 2011, Shinneman and McIlroy 2019). Given the evidence that precipitation is a critical driver of aspen performance, it is slightly surprising that only two precipitation related variables, of small effect size, were present among our best

performing models. It may be that our climate summaries failed to accurately reflect periods of severe drought, which could have been brief relative to the duration over which climate values were averaged (15 to 18 years in the case of mortality predictor variables, 10 to 13 years in the case of predictors of all other response variables).

4.6 Conclusions

We have documented high rates of mortality relative to recruitment in quaking aspen, a widespread, foundation tree species. This demographic decline over the past decade was persistent across a large geographic area, that constitutes the more arid parts of aspen's range. However, aspen performance was highly variable at small spatial scales, leading us to conclude that consideration of landscape-scale factors — including stand structure, topography, and local climate — will be essential for predicting the future dynamics of aspen. We found that aspen stands with fewer, smaller trees exhibited faster growth and recruitment rates, and that stands that experienced initial high levels of dieback continued to deteriorate. Furthermore, given that 1) we found a surprising negative relationship between mortality and VPD deviation (a variable strongly influenced by temperature), 2) variables heavily influenced by temperature had a strong association with every demographic rate and every size class of aspen we modeled, and 3) the results found by previous studies with regards to temperature–growth rate relationships and temperature–immature aspen performance relationships are mixed — we suggest that temperature is a critical driver of aspen performance and that the complex nature of this relationship is not yet fully understood. In order to fully elucidate temperature–aspen performance relationships, we suggest that future studies should 1)

investigate the possibility of a non-monotonic relationship between temperature and aspen performance; 2) distinguish between warming trends in climate and discrete extreme heat events; 3) incorporate interactions between temperature, water availability, and evaporative demand; and 4) consider the annual timing of these factors. This study provides evidence that aspen, in the more arid portions of its range, is contributing to an increasing worldwide pattern of tree decline. While tree decline is a global phenomenon, our work demonstrates the importance of local-scale factors in contributing to the risk of different populations.

Literature Cited

- Abatzoglou, J. T., S. Z. Dobrowski, S. A. Parks, and K. C. Hegewisch. 2018. TerraClimate, a high-resolution global dataset of monthly climate and climatic water balance from 1958–2015. *Scientific Data* 5:170191.
- Allen, C. D., D. D. Breshears, and N. G. McDowell. 2015. On underestimation of global vulnerability to tree mortality and forest die-off from hotter drought in the Anthropocene. *Ecosphere* 6(8):1–55.
- Allen, C. D., A. K. Macalady, H. Chenchouni, D. Bachelet, N. McDowell, M. Vennetier, T. Kitzberger, A. Rigling, D. D. Breshears, E. H. Hogg, P. Gonzalez, R. Fensham, Z. Zhang, J. Castro, N. Demidova, J.-H. Lim, G. Allard, S. W. Running, A. Semerci, and N. Cobb. 2010. A global overview of drought and heat-induced tree mortality reveals emerging climate change risks for forests. *Forest Ecology and Management* 259:660–684.
- Anderegg, L. D. L., W. R. L. Anderegg, J. Abatzoglou, A. M. Hausladen, and J. A. Berry. 2013a. Drought characteristics' role in widespread aspen forest mortality across Colorado, USA. *Global Change Biology* 19:1526–1537.
- Anderegg, W. R. L., A. Flint, C. Huang, L. Flint, J. A. Berry, F. W. Davis, J. S. Sperry, and C. B. Field. 2015. Tree mortality predicted from drought-induced vascular damage. *Nature Geoscience* 8:367–371.
- Anderegg, W. R. L., J. M. Kane, and L. D. L. Anderegg. 2013b. Consequences of widespread tree mortality triggered by drought and temperature stress. *Nature Climate Change* 3:30–36.
- Anderegg, W. R. L., L. Plavcová, L. D. L. Anderegg, U. G. Hacke, J. A. Berry, and C. B. Field. 2013c. Drought's legacy: multiyear hydraulic deterioration underlies widespread aspen forest die-off and portends increased future risk. *Global Change Biology* 19:1188–1196.
- Arthur, A. D., J. Li, S. Henry, and S. A. Cunningham. 2010. Influence of woody vegetation on pollinator densities in oilseed Brassica fields in an Australian temperate landscape. *Basic and Applied Ecology* 11:406–414.
- Barton, K. 2019. MuMIn: multi-model inference.

- Bell, D. M., J. B. Bradford, and W. K. Lauenroth. 2014. Forest stand structure, productivity, and age mediate climatic effects on aspen decline. *Ecology* 95:2040–2046.
- Bell, D. M., J. B. Bradford, and W. K. Lauenroth. 2015. Scale dependence of disease impacts on quaking aspen (*Populus tremuloides*) mortality in the southwestern United States. *Ecology* 96:1835–1845.
- Benjamini, Y., and Y. Hochberg. 1995. Controlling the false discovery rate: a practical and powerful approach to multiple testing. *Journal of the Royal Statistical Society: Series B (Methodological)* 57:289–300.
- Berrill, J.-P., and C. M. Dagley. 2012. Geographic patterns and stand variables influencing growth and vigor of *Populus tremuloides* in the Sierra Nevada (USA). *ISRN Forestry* 2012:1–9.
- Beschta, R. L., and W. J. Ripple. 2009. Large predators and trophic cascades in terrestrial ecosystems of the western United States. *Biological Conservation* 142:2401–2414.
- Bonan, G. B. 2008. Forests and climate change: forcings, feedbacks, and the climate benefits of forests. *Science* 320:1444–1449.
- Breshears, D. D., N. S. Cobb, P. M. Rich, K. P. Price, C. D. Allen, R. G. Balice, W. H. Romme, J. H. Kastens, M. L. Floyd, J. Belnap, J. J. Anderson, O. B. Myers, and C. W. Meyer. 2005. Regional vegetation die-off in response to global-change-type drought. *Proceedings of the National Academy of Sciences* 102:15144–15148.
- Bretfeld, M., S. B. Franklin, and R. K. Peet. 2016. A multiple-scale assessment of long-term aspen persistence and elevational range shifts in the Colorado Front Range. *Ecological Monographs* 86:244–260.
- Brodie, J., E. Post, F. Watson, and J. Berger. 2012. Climate change intensification of herbivore impacts on tree recruitment. *Proceedings of the Royal Society B: Biological Sciences* 279:1366–1370.
- Brown, K., A. J. Hansen, R. E. Keane, and L. J. Graumlich. 2006. Complex interactions shaping aspen dynamics in the Greater Yellowstone Ecosystem. *Landscape Ecology* 21:933–951.

- Callahan, C. M., C. A. Rowe, R. J. Ryel, J. D. Shaw, M. D. Madritch, and K. E. Mock. 2013. Continental-scale assessment of genetic diversity and population structure in quaking aspen (*Populus tremuloides*). *Journal of Biogeography* 40:1780–1791.
- Canham, C. D., M. J. Papaik, M. Uriarte, W. H. McWilliams, J. C. Jenkins, and M. J. Twery. 2006. Neighborhood analyses of canopy tree competition along environmental gradients in New England forests. *Ecological Applications* 16:540–554.
- Chen, L., J.-G. Huang, S. A. Alam, L. Zhai, A. Dawson, K. J. Stadt, and P. G. Comeau. 2017. Drought causes reduced growth of trembling aspen in western Canada. *Global Change Biology* 23:2887–2902.
- Chen, L., J.-G. Huang, A. Dawson, L. Zhai, K. J. Stadt, P. G. Comeau, and C. Whitehouse. 2018. Contributions of insects and droughts to growth decline of trembling aspen mixed boreal forest of western Canada. *Global Change Biology* 24:655–667.
- Clement, M. J., L. E. Harding, R. W. Lucas, and E. S. Rubin. 2019. The relative importance of biotic and abiotic factors influencing aspen recruitment in Arizona. *Forest Ecology and Management* 441:32–41.
- Cluck, D. R. 2011. Forest health survey of northeastern California aspen (No. NE-SPR-12-01). Pages 1-33. U.S. Forest Service, Susanville, California.
- Cohen, W. B., Z. Yang, S. V. Stehman, T. A. Schroeder, D. M. Bell, J. G. Masek, C. Huang, and G. W. Meigs. 2016. Forest disturbance across the conterminous United States from 1985–2012: the emerging dominance of forest decline. *Forest Ecology and Management* 360:242–252.
- Dilts, T. E. 2019. Topography tools for ArcGIS 10.3. University of Nevada Reno.
- Dudley, M. M., K. S. Burns, and W. R. Jacobi. 2015. Aspen mortality in the Colorado and southern Wyoming Rocky Mountains: Extent, severity, and causal factors. *Forest Ecology and Management* 353:240–259.
- Eisenberg, C., S. T. Seager, and D. E. Hibbs. 2013. Wolf, elk, and aspen food web relationships: Context and complexity. *Forest Ecology and Management* 299:70–80.

- Foote, K. C., and M. Schaedle. 1978. Contribution of aspen bark photosynthesis to the energy balance of the stem. *Forest Science* 24:569–573.
- Guyon, J., and J. Hoffman. 2011. Survey of aspen dieback in the intermountain region (R4-OFO-Report 11-01). Pages 1-20. U.S. Forest Service.
- Hanna, P., and D. Kulakowski. 2012. The influences of climate on aspen dieback. *Forest Ecology and Management* 274:91–98.
- Hansen, W. D. 2016. Shifting ecological filters mediate postfire expansion of seedling aspen (*Populus tremuloides*) in Yellowstone. *Forest Ecology and Management*:13.
- Hartig, F. 2020. DHARMA: residual diagnostics for hierarchical (multi-level / mixed) regression models.
- Hember, R. A., W. A. Kurz, and N. C. Coops. 2017. Relationships between individual-tree mortality and water-balance variables indicate positive trends in water stress-induced tree mortality across North America. *Global Change Biology* 23:1691–1710.
- Hervé, M. 2020. RVAideMemoire: testing and plotting procedures for biostatistics.
- Hijmans, R. J., S. E. Cameron, J. L. Parra, P. G. Jones, and A. Jarvis. 2005. Very high resolution interpolated climate surfaces for global land areas. *International Journal of Climatology* 25:1965–1978.
- Hogg, E. H., J. P. Brandt, and B. Kochtubajda. 2002. Growth and dieback of aspen forests in northwestern Alberta, Canada, in relation to climate and insects. *Canadian Journal of Forest Research* 32:823–832.
- Huang, C.-Y., and W. R. L. Anderegg. 2012. Large drought-induced aboveground live biomass losses in southern Rocky Mountain aspen forests. *Global Change Biology* 18:1016–1027.
- Jones, B. E., T. H. Rickman, A. Vazquez, Y. Sado, and K. W. Tate. 2005. Removal of encroaching conifers to regenerate degraded aspen stands in the Sierra Nevada. *Restoration Ecology* 13:373–379.

- Kane, J. M., T. E. Kolb, and J. D. McMillin. 2014. Stand-scale tree mortality factors differ by site and species following drought in southwestern mixed conifer forests. *Forest Ecology and Management* 330:171–182.
- Kashian, D. M., W. H. Romme, and C. M. Regan. 2007. Reconciling divergent interpretations of quaking aspen decline on the northern Colorado front range. *Ecological Applications* 17:1296–1311.
- Kaye, M. W. 2011. Mesoscale synchrony in quaking aspen establishment across the interior western US. *Forest Ecology and Management* 262:389–397.
- Kaye, M. W., D. Binkley, and T. J. Stohlgren. 2005. Effects of conifers and elk browsing on quaking aspen forests in the central Rocky Mountains, USA. *Ecological Applications* 15:1284–1295.
- Keenan, R. J., G. A. Reams, F. Achard, J. V. de Freitas, A. Grainger, and E. Lindquist. 2015. Dynamics of global forest area: Results from the FAO Global Forest Resources Assessment 2015. *Forest Ecology and Management* 352:9–20.
- Kemperman, J. A., and B. V. Barnes. 1976. Clone size in American aspens. *Canadian Journal of Botany* 54:2603–2607.
- Krasnow, K. D., and S. L. Stephens. 2015. Evolving paradigms of aspen ecology and management: impacts of stand condition and fire severity on vegetation dynamics. *Ecosphere* 6:art12.
- Kweon, D., and P. G. Comeau. 2019. Relationships between tree survival, stand structure and age in trembling aspen dominated stands. *Forest Ecology and Management* 438:114–122.
- Liaw, A., and M. Wiener. 2002. Classification and Regression by randomForest.
- Luo, Y., and H. Y. H. Chen. 2013. Observations from old forests underestimate climate change effects on tree mortality. *Nature Communications* 4.
- Luo, Y., and H. Y. H. Chen. 2015. Climate change-associated tree mortality increases without decreasing water availability. *Ecology Letters* 18:1207–1215.

- van Mantgem, P. J., N. L. Stephenson, J. C. Byrne, L. D. Daniels, J. F. Franklin, P. Z. Fule, M. E. Harmon, A. J. Larson, J. M. Smith, A. H. Taylor, and T. T. Veblen. 2009. Widespread increase of tree mortality rates in the western United States. *Science* 323:521–524.
- Marchetti, S. B., J. J. Worrall, and T. Eager. 2011. Secondary insects and diseases contribute to sudden aspen decline in southwestern Colorado, USA. *Canadian Journal of Forest Research* 41:2315–2325.
- Martin, T. E., and J. L. Maron. 2012. Climate impacts on bird and plant communities from altered animal–plant interactions. *Nature Climate Change* 2:195–200.
- McCune, B., and D. Keon. 2002. Equations for potential annual direct incident radiation and heat load. *Journal of Vegetation Science* 13:603–606.
- McDowell, N. G., D. J. Beerling, D. D. Breshears, R. A. Fisher, K. F. Raffa, and M. Stitt. 2011. The interdependence of mechanisms underlying climate-driven vegetation mortality. *Trends in Ecology & Evolution* 26:523–532.
- McIlroy, S. K., and D. J. Shinneman. 2020. Post-fire aspen (*Populus tremuloides*) regeneration varies in response to winter precipitation across a regional climate gradient. *Forest Ecology and Management* 455:117681.
- Michaelian, M., E. H. Hogg, R. J. Hall, and E. Arsenault. 2011. Massive mortality of aspen following severe drought along the southern edge of the Canadian boreal forest. *Global Change Biology* 17:2084–2094.
- Millar, C. I., and N. L. Stephenson. 2015. Temperate forest health in an era of emerging megadisturbance. *Science* 349:823–826.
- Miller, M. F., T. J. Svejcar, and J. A. Rose. 2000. Impacts of western juniper on plant community composition and structure. *Journal of Range Management* 53:574–585.
- Mock, K. E., C. A. Rowe, M. B. Hooten, J. Dewoody, and V. D. Hipkins. 2008. Clonal dynamics in western North American aspen (*Populus tremuloides*). *Molecular Ecology* 17:4827–4844.

- Nelson, D. W., and L. E. Sommers. 2018. Total Carbon, Organic Carbon, and Organic Matter. Pages 961–1010 in D. L. Sparks, A. L. Page, P. A. Helmke, R. H. Loeppert, P. N. Soltanpour, M. A. Tabatabai, C. T. Johnston, and M. E. Sumner, editors. SSSA Book Series. Soil Science Society of America, American Society of Agronomy, Madison, WI, USA.
- Pan, Y., R. A. Birdsey, J. Fang, R. Houghton, P. E. Kauppi, W. A. Kurz, O. L. Phillips, A. Shvidenko, S. L. Lewis, J. G. Canadell, P. Ciais, R. B. Jackson, S. W. Pacala, A. D. McGuire, S. Piao, A. Rautiainen, S. Sitch, and D. Hayes. 2011. A large and persistent carbon sink in the world's forests. *Science* 333:988–993.
- Peng, C., Z. Ma, X. Lei, Q. Zhu, H. Chen, W. Wang, S. Liu, W. Li, X. Fang, and X. Zhou. 2011. A drought-induced pervasive increase in tree mortality across Canada's boreal forests. *Nature Climate Change* 1:467–471.
- Perala, D. A., R. M. Burns, and B. Honkala. 1990. *Populus tremuloides* Michx.-quaking aspen. *Silvics of North America: hardwoods*:555–569.
- Peterson, E. B., and N. M. Peterson. 1992. Ecology, management, and use of aspen and balsam poplar in the prairie provinces, Canada (No. Special Report 1). Northwest Region, Northern Forestry Centre, Edmonton, Alberta, Canada: Forestry Canada.
- Pierce, A. D., and A. H. Taylor. 2010. Competition and regeneration in quaking aspen-white fir (*Populus tremuloides* - *Abies concolor*) forests in the Northern Sierra Nevada, USA. *Journal of Vegetation Science* 21:507–519.
- R Core Team. 2020. R: A language and environment for statistical computing. R Foundation for Statistical Computing, Vienna, Austria.
- Rehfeldt, G. E., D. E. Ferguson, and N. L. Crookston. 2009. Aspen, climate, and sudden decline in western USA. *Forest Ecology and Management* 258:2353–2364.
- Rhodes, A. C., H. Y. Wan, and S. B. St. Clair. 2017. Herbivory impacts of elk, deer and cattle on aspen forest recruitment along gradients of stand composition, topography and climate. *Forest Ecology and Management* 397:39–47.
- Richards, S. A. 2005. Testing ecological theory using the information-theoretic approach: examples and cautionary results. *Ecology* 86:2805–2814.

- Rogers, B. M., K. Solvik, E. H. Hogg, J. Ju, J. G. Masek, M. Michaelian, L. T. Berner, and S. J. Goetz. 2018. Detecting early warning signals of tree mortality in boreal North America using multiscale satellite data. *Global Change Biology* 24:2284–2304.
- Rogers, P. C., B. D. Pinno, J. Šebesta, B. R. Albrechtsen, G. Li, N. Ivanova, A. Kusbach, T. Kuuluvainen, S. M. Landhäusser, H. Liu, T. Myking, P. Pulkkinen, Z. Wen, and D. Kulakowski. 2020. A global view of aspen: Conservation science for widespread keystone systems. *Global Ecology and Conservation* 21:e00828.
- Schielzeth, H. 2010. Simple means to improve the interpretability of regression coefficients. *Methods in Ecology and Evolution* 1:103–113.
- Seager, S. T., C. Eisenberg, and S. B. St. Clair. 2013. Patterns and consequences of ungulate herbivory on aspen in western North America. *Forest Ecology and Management* 299:81–90.
- Seidl, R., M.-J. Schelhaas, and M. J. Lexer. 2011. Unraveling the drivers of intensifying forest disturbance regimes in Europe: drivers of forest disturbance intensification. *Global Change Biology* 17:2842–2852.
- Shinneman, D. J., W. L. Baker, P. C. Rogers, and D. Kulakowski. 2013. Fire regimes of quaking aspen in the Mountain West. *Forest Ecology and Management* 299:22–34.
- Shinneman, D. J., and S. K. McIlroy. 2019. Climate and disturbance influence self-sustaining stand dynamics of aspen (*Populus tremuloides*) near its range margin. *Ecological Applications* 29.
- St. Clair, S. B., X. Cavard, and Y. Bergeron. 2013. The role of facilitation and competition in the development and resilience of aspen forests. *Forest Ecology and Management* 299:91–99.
- Trugman, A. T., D. Medvigy, W. R. L. Anderegg, and S. W. Pacala. 2018. Differential declines in Alaskan boreal forest vitality related to climate and competition. *Global Change Biology* 24:1097–1107.
- Trumbore, S., P. Brando, and H. Hartmann. 2015. Forest health and global change. *Science* 349:814–818.

- Turner, M. G., W. H. Romme, R. A. Reed, and G. A. Tuskan. 2003. Post-fire aspen seedling recruitment across the Yellowstone (USA) Landscape. *Landscape Ecology* 18:127–140.
- White, C. A., M. C. Feller, and S. Bayley. 2003. Predation risk and the functional response of elk–aspen herbivory. *Forest Ecology and Management* 181:77–97.
- Worrall, J. J., L. Egeland, T. Eager, R. A. Mask, E. W. Johnson, P. A. Kemp, and W. D. Shepperd. 2008. Rapid mortality of *Populus tremuloides* in southwestern Colorado, USA. *Forest Ecology and Management* 255:686–696.
- Worrall, J. J., A. G. Keck, and S. B. Marchetti. 2015. *Populus tremuloides* stands continue to deteriorate after drought-incited sudden aspen decline. *Canadian Journal of Forest Research* 45:1768–1774.
- Worrall, J. J., S. B. Marchetti, L. Egeland, R. A. Mask, T. Eager, and B. Howell. 2010. Effects and etiology of sudden aspen decline in southwestern Colorado, USA. *Forest Ecology and Management* 260:638–648.
- Worrall, J. J., G. E. Rehfeldt, A. Hamann, E. H. Hogg, S. B. Marchetti, M. Michaelian, and L. K. Gray. 2013. Recent declines of *Populus tremuloides* in North America linked to climate. *Forest Ecology and Management* 299:35–51.
- Yang, J., P. J. Weisberg, D. J. Shinneman, T. E. Dilts, S. L. Earnst, and R. M. Scheller. 2015. Fire modulates climate change response of simulated aspen distribution across topoclimatic gradients in a semi-arid montane landscape. *Landscape Ecology* 30:1055–1073.
- Zegler, T. J., M. M. Moore, M. L. Fairweather, K. B. Ireland, and P. Z. Fulé. 2012. *Populus tremuloides* mortality near the southwestern edge of its range. *Forest Ecology and Management* 282:196–207.
- Zhang, J., S. Huang, and F. He. 2015. Half-century evidence from western Canada shows forest dynamics are primarily driven by competition followed by climate. *Proceedings of the National Academy of Sciences* 112:4009–4014.

Figure Legends

Figure 1. Locations of the 184 aspen monitoring plots in the western United States. Plots are colored according to their assigned geographical region.

Figure 2. Mean (\pm SE) stem density of aspen (a) saplings, (b) juveniles, and (c) suckers in 2019, by region. Means denoted by a different letter indicate significant differences between regions.

Figure 3. Mean (\pm SE) annual percent change in live basal area of aspen and conifer mature trees during the study period, by region. Means denoted by a different letter indicate significant differences between aspen and conifers and/or between regions.

Figure 4. Marginal effect plots of the best-performing predictors of aspen mortality rate. Panels show the predicted mean and 95% confidence interval of annual percent mortality of aspen as a function of (a) mean initial canopy dieback rating of aspen, (b) annual vapor pressure deficit deviation, (c) annual temperature range, (d) total dead basal area of all species in the initial sampling, (e) potential incident solar radiation, and (f) annual precipitation deviation.

Figure 5. Marginal effect plots of the best-performing predictors of aspen recruitment rate. Panels show the predicted mean and 95% confidence interval of annual percent recruitment of aspen into the mature stem size class as a function of (a) live aspen basal area in the initial sampling, (b) mean spring snow water equivalent, and (c) mean annual PDSI.

Figure 6. Marginal effect plots of the best-performing predictors of aspen growth rate. Panels show the predicted mean and 95% confidence interval of growth rate (mean percent change in individual basal area) as a function of (a) total live basal area (of all species in the initial sampling), (b) mean summer vapor pressure, (c) mean annual high temperature, (d) the standard deviation of individual aspens' basal areas in the initial sampling, and (e) topographic position index (calculated with a 100 m radius neighborhood).

Figure 7. Marginal effect plots of the best-performing predictors of aspen sapling density. Panels show the predicted mean and 95% confidence interval of sapling density as a function of (a) the number of aspen suckers plus juveniles present in the initial sampling, (b) mean summer climatic water deficit, and (c) the number of mature trees (all species) present in the initial sampling. Panel (b) illustrates the interaction between mean summer climatic water deficit and total live basal area (of all species in the initial sampling) by showing the marginal effect of mean climatic water deficit on aspen sapling density at three different values of basal area: one standard deviation below the mean ($9.5 \text{ m}^2\text{ha}^{-1}$), the mean value ($33.4 \text{ m}^2\text{ha}^{-1}$), and one standard deviation above the mean ($57.3 \text{ m}^2\text{ha}^{-1}$).

Figure 8. Marginal effect plots of the best-performing predictors of aspen juvenile density. Panels show the predicted mean and 95% confidence interval of juvenile density as a function of (a) elevation, (b) summer climatic water deficit deviation, and (c) winter high temperature deviation.

Figure 9. Marginal effect plots of the best-performing predictors of aspen sucker density. Panels show the predicted mean and 95% confidence interval of sucker density as a function of whether a stream was present in the plot and at the time of the final sampling and (a) Mean winter vapor pressure deficit and (b) seasonality of precipitation on sucker density.

Figure S1. Correlation matrix of aspen response variables. Values represent Kendall's τ_b correlation coefficients. Periods indicate $0.5 \leq p < 0.1$, single asterisks indicate $0.01 \leq p < 0.05$, double asterisks indicate $0.001 \leq p < 0.01$, and triple asterisks indicate $p < 0.001$. Larger dots with darker tone represent stronger correlations. Blue dots indicate positive correlations, red dots indicate negative correlations.

Figure S2. Correlation matrix of predictor variables. Includes all predictor variables present in our best-performing models, as well as mean high temperature for spring, summer, fall, and winter, and mean individual aspen BA. Values shown are pairwise Pearson correlation coefficients. Significance statistics for correlations were not calculated. Larger dots with darker tone represent stronger correlations. Blue dots indicate positive correlations, red dots indicate negative correlations.

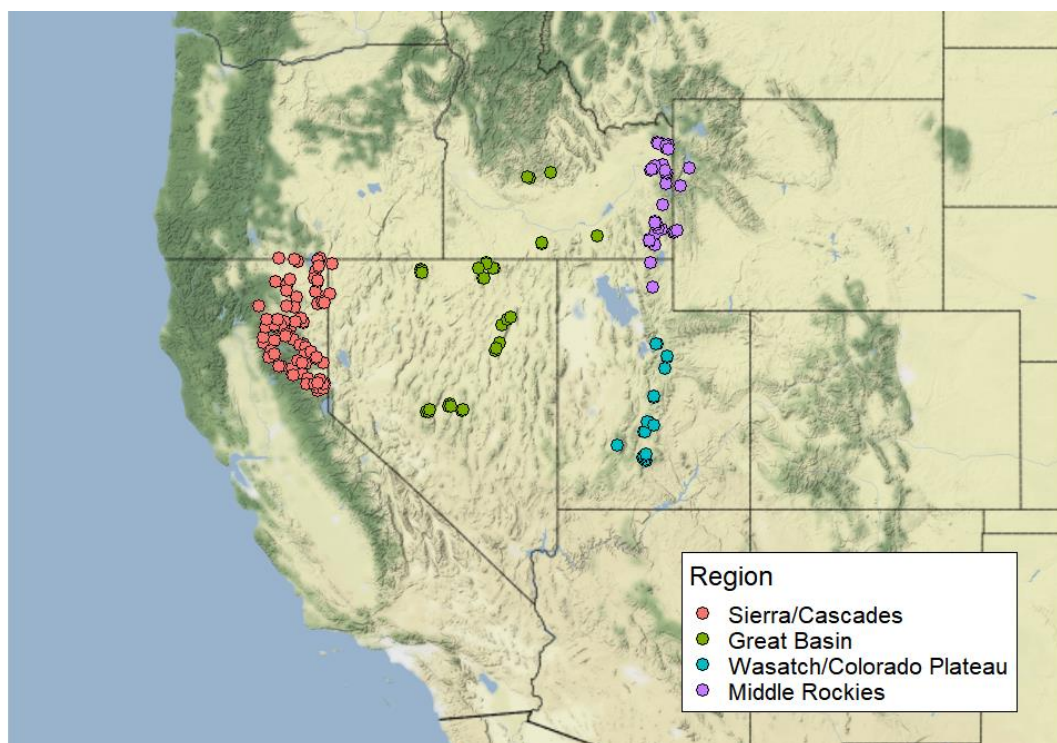
Figure 1

Figure 2

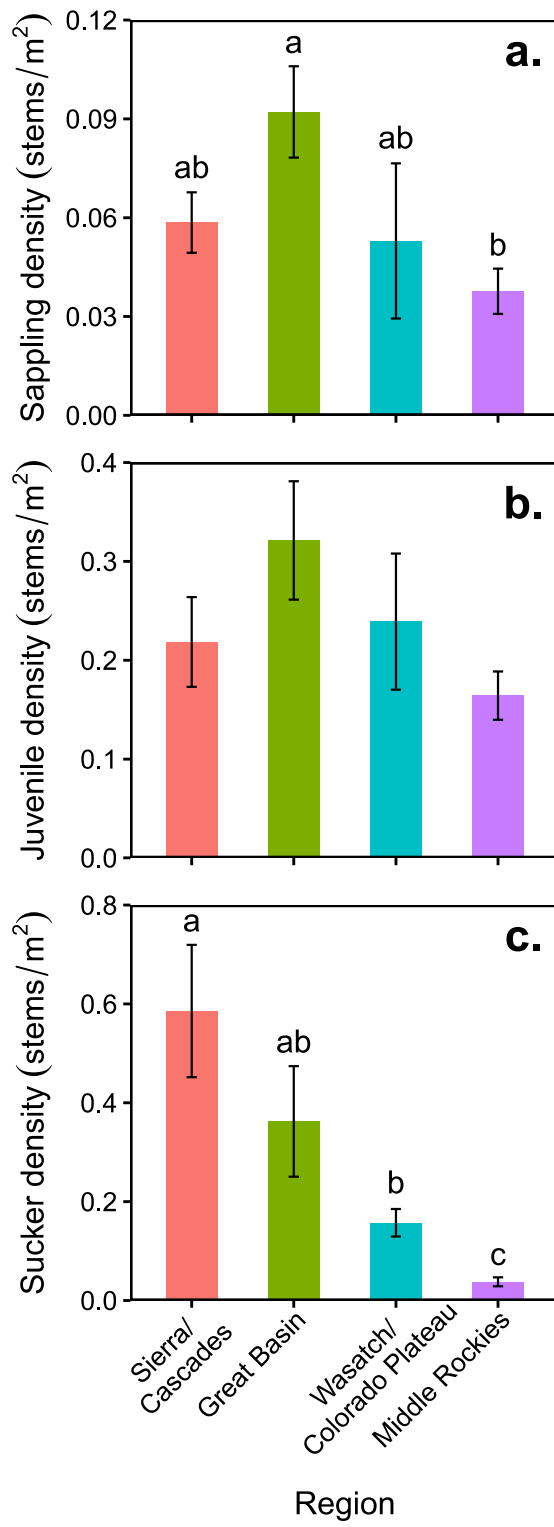


Figure 3

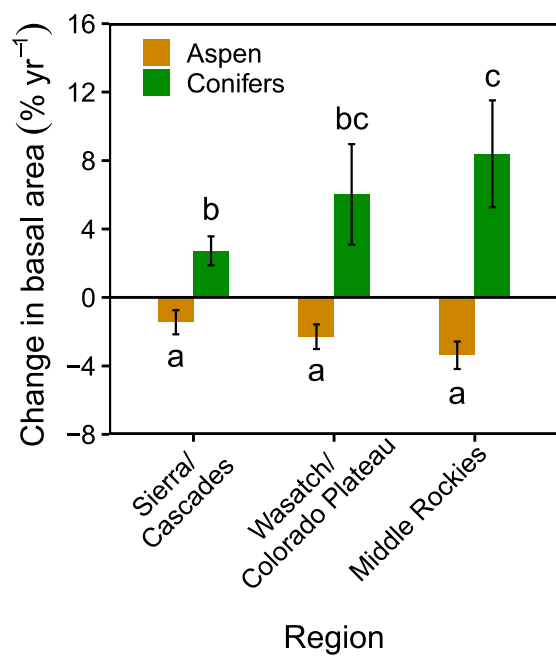


Figure 4

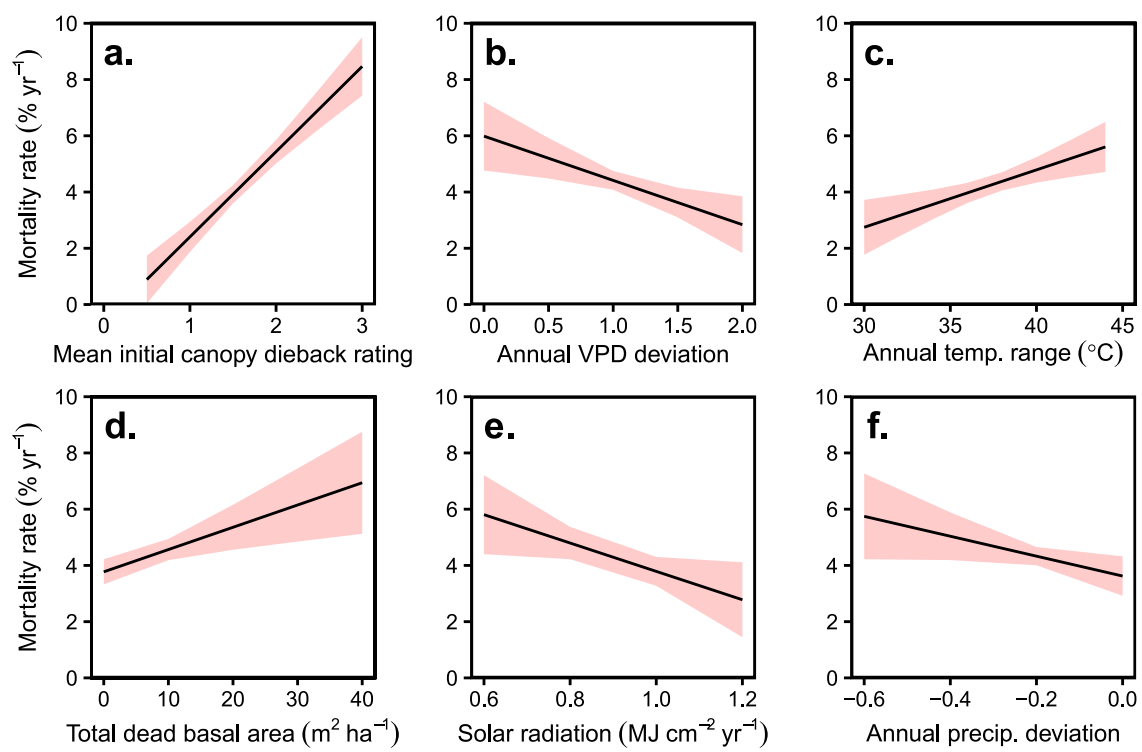


Figure 5

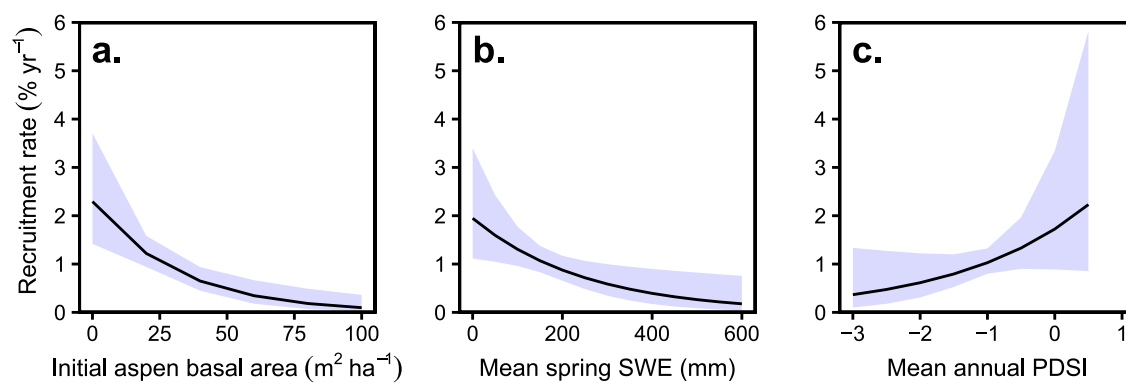


Figure 6

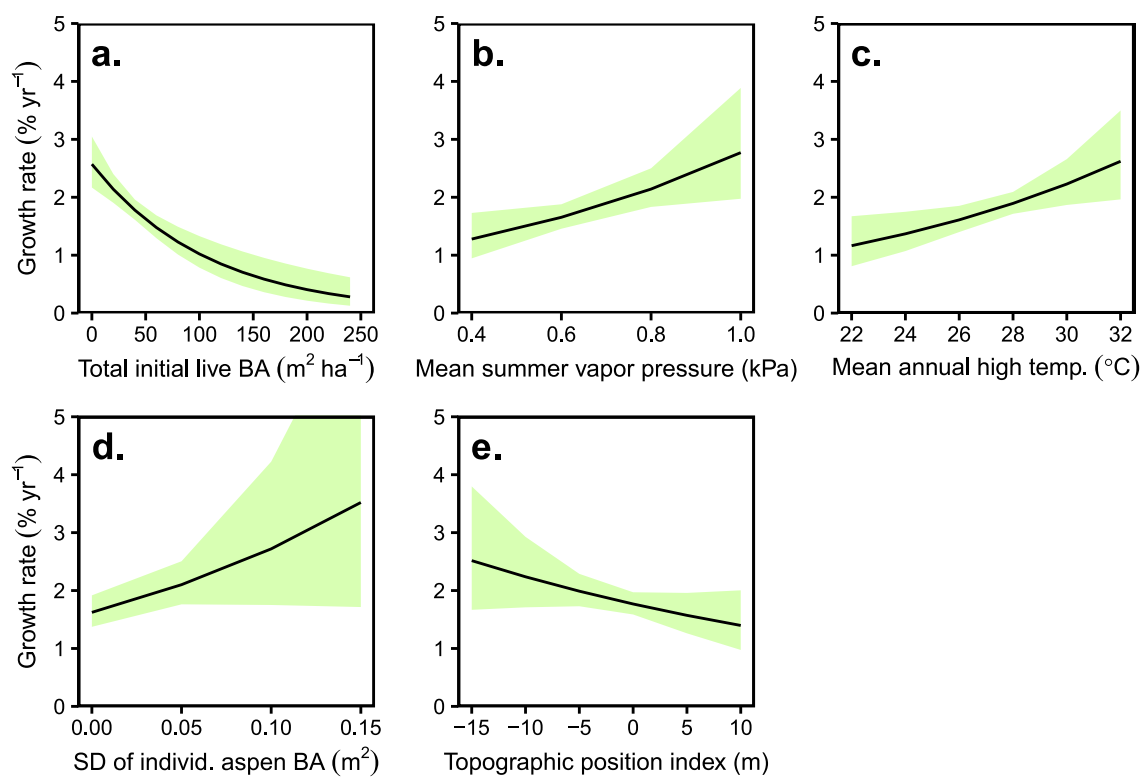


Figure 7

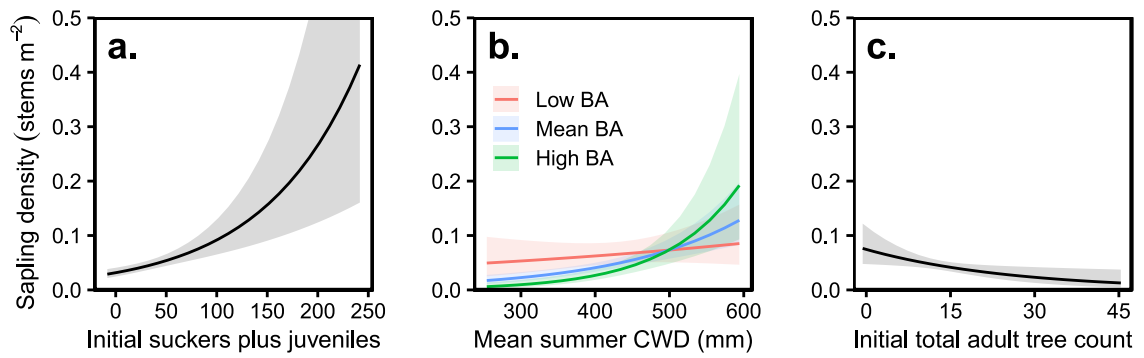


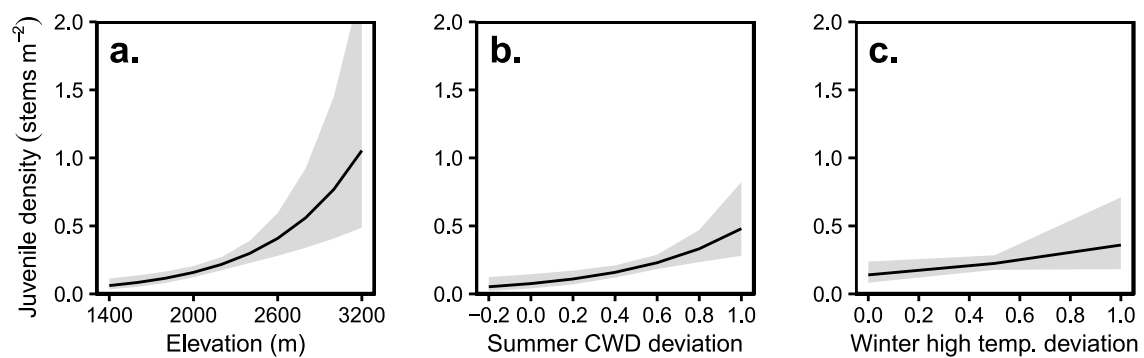
Figure 8

Figure 9

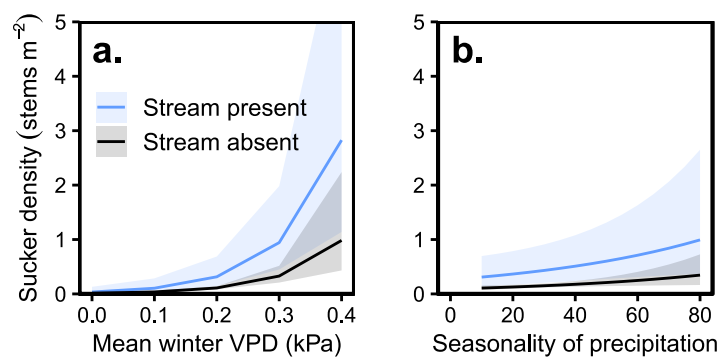


Figure S1

	Annual percent mortality	Annual percent adult recruitment	Growth rate	Sapling density	Juvenile density	Sucker density
Annual percent mortality	1	-0.08 [.]	-0.07	0.03	0.18 ^{**}	-0.04
Annual percent adult recruitment	-0.08 [.]	1	0.25 ^{***}	0.29 ^{***}	-0.05	-0.02
Growth rate	-0.07	0.25 ^{***}	1	0.24 ^{***}	-0.02	-0.15 [*]
Sapling density	0.03	0.29 ^{***}	0.24 ^{***}	1	0.3 ^{***}	0.08 [.]
Juvenile density	0.18 ^{**}	-0.05	-0.02	0.3 ^{***}	1	0.38 ^{***}
Sucker density	-0.04	-0.02	-0.15 [*]	0.08 [.]	0.38 ^{***}	1

Figure S2

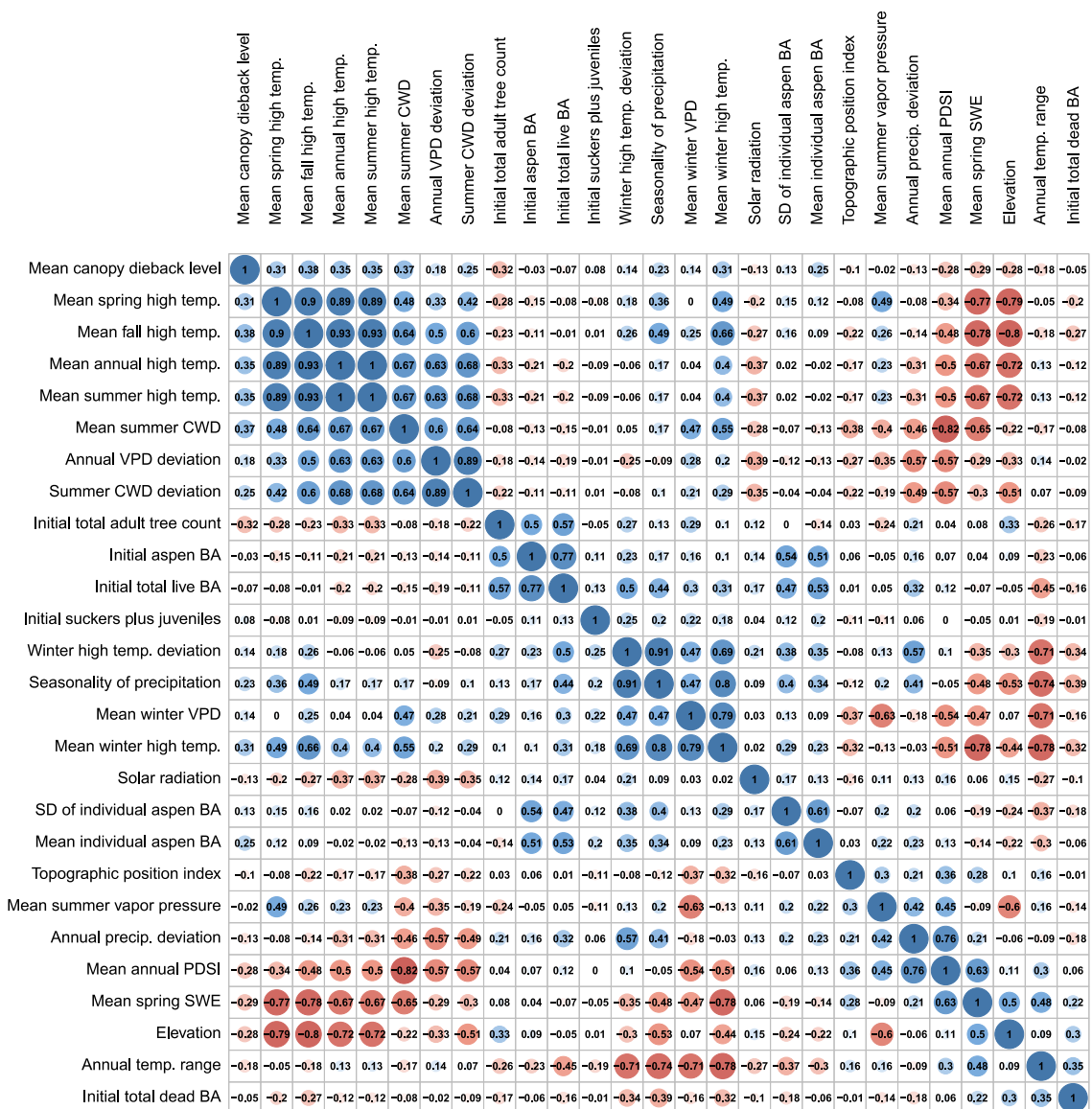


Table 1. Climate variables included in random forest stepwise selection process for modeling aspen mortality, mature stem recruitment, growth rate, and sapling, juvenile, and sucker densities. (a) Variables derived from monthly climate data provided by TerraClimate. (b) Variables included from WorldClim climate normals.

a. Climate summaries calculated from monthly TerraClimate data		
Variable name	Formula	Description
Mean annual value or Mean seasonal value	$\frac{\sum_{i=t_1}^{t_2} X_i}{t_2 - t_1}$	Annual or seasonal climate values averaged over time period of interest
Mean annual difference from normal	$\frac{\sum_{i=t_1}^{t_2} X_i - \bar{X}_{\text{norm}}}{t_2 - t_1}$	Annual climate values centered on the 30-year normal mean, then averaged over time period of interest
Annual deviation or Seasonal deviation	$\frac{\sum_{i=t_1}^{t_2} (X_i - \bar{X}_{\text{norm}}) / \sigma_{\text{norm}}}{t_2 - t_1}$	Annual or seasonal climate values centered and scaled by the mean and standard deviation, respectively, of the 30-year normal, then averaged over time period of interest
Minimum PDSI	$\min\{X_{t_1}, \dots, X_{t_2}\}$	Minimum value of annual or seasonal PDSI that occurred during time period of interest
Maximum summer high temperature	$\max\{X_{t_1}, \dots, X_{t_2}\}$	Maximum value of summer high temperature that occurred during time period of interest
b. Predictor variables included from WorldClim normals		
Variable name	Description	
Diurnal temperature range	The mean of monthly maximum temperature minus minimum temperature	
Annual temperature range	The maximum temperature of the warmest month minus the minimum temperature of the coldest month	
Isothermality	The ratio of Diurnal temperature range to Annual temperature range, scaled from zero to 100	
Seasonality of temperature	The standard deviation of monthly temperature multiplied by 100	
Seasonality of precipitation	The coefficient of variation of monthly precipitation	

Note: For the first time period of interest, t_1 equals the year of plot establishment and t_2 equals the year of plot resampling. For the second time period of interest, t_1 equals five years prior to the year of plot establishment and t_2 equals the year of plot resampling. For annual summaries, X represents the mean annual value for vapor pressure, VPD, daily high temperature, and PDSI, and the cumulative annual value for precipitation accumulation, CWD, and SWE. For seasonal summaries, X represents the mean of monthly values over a single season for vapor pressure, VPD, daily high temperature, and PDSI, and the sum of monthly values over a single season for precipitation accumulation, CWD, and SWE. The mean of X over the 30-year normal (1960-1990) is represented by \bar{X}_{norm} and the standard deviation by σ_{norm} .

Table 2. Topographic variables included in random forest stepwise selection process for modeling aspen mortality, mature stem recruitment, growth rate, and sapling, juvenile, and sucker densities.

Variable name	Units	Description
Stream presence	Unitless	A binary predictor indicating if a stream with water in it was present within the border of the plot at the time of the final sampling
Elevation	Meters	The elevation of the plot center
Slope	%	The average slope of the plot
Folded aspect (about 0° line)	Degrees	“Aspect [...] ‘folded’ about the north-south line, rescaling 0-360° to 0-180°, such that NE = NW, E = W, etc.” (McCune and Keon 2002)
Folded aspect (about 45° line)	Degrees	A plot’s aspect ‘folded’ about the northeast-southwest line
Potential solar radiation	$\frac{MJ}{cm^2 yr}$	Estimates potential annual direct incident radiation as a function of slope, folded aspect (about 0° line), and latitude as per McCune and Keon (2002), table 2, equation 3.
Heat load index	Unitless	Analogous to potential incident solar radiation, but uses aspect folded about 45° line as an input rather than aspect folded about 0° line. Calculated as per McCune and Keon (2002), table 2, equation 3.
Topographic wetness index (30 m resolution)	Unitless	A proxy for cold air drainage and runoff accumulation based on the local slope and upslope area within the watershed such that points with shallower slope and greater upslope area will have higher index values. Calculated from 30 m resolution USGS DEMs using ‘Topography tools for ArcGIS 10.3 and earlier’ (Dilts 2019) running in arcMAP version 10.6.1.
Topographic wetness index (90 m resolution)	Unitless	Topographic wetness index calculated from 90 m resolution USGS DEMs using ‘Topography tools for ArcGIS 10.3 and earlier’ (Dilts 2019) running in arcMAP version 10.6.1.
Topographic position index	Meters	The elevation of a point relative to the average elevation of the surrounding neighborhood. The index was calculated for four circular neighborhoods of different sizes: 100 m radius, 500m radius, 2.25 km radius, and 20 km radius. The 100 m through 2.25 km radius neighborhood index values were calculated from 10 m resolution USGS DEMs and the 20 km radius neighborhood index value was calculated from 90 m resolution USGS DEMs using ‘Topography tools for ArcGIS 10.3 and earlier’ (Dilts 2019) running in arcMAP version 10.6.1.
Curvature	$\frac{\%}{meter}$	Describes the degree of concavity (positive values) or convexity (negative values) of a hill slope (i.e. change in percent slope per meter). Calculated from 10 m resolution USGS DEMs using the curvature function in arcMAP version 10.6.1.
Profile curvature	$\frac{\%}{meter}$	Curvature calculated in the direction parallel to the slope. Calculated from 10 m resolution USGS DEMs using the curvature function in arcMAP version 10.6.1.
Planform curvature	$\frac{\%}{meter}$	Curvature calculated in the direction perpendicular to the direction of maximum slope. Calculated from 10 m resolution USGS DEMs using the curvature function in arcMAP version 10.6.1.

Table 3. Stand structure and composition variables included in random forest stepwise selection process for modeling aspen mortality, recruitment, growth rate, and sapling density. Juvenile and sucker density stepwise selection models include all variables except ‘Initial suckers plus juveniles’.

Metric name	Units	Description	Summarized for each of the following stand components
Initial basal area	m ² /ha	Basal area of mature trees present in plot during initial sampling	All live mature trees All standing dead mature trees Live mature aspen Dead mature aspen Live mature conifers Dead mature conifers Live mature non-aspen hardwoods [†] Dead mature non-aspen hardwoods [†]
Initial tree count	Unitless	Number of mature trees present in plot during initial sampling	All live mature trees
Initial mean individual basal area	m ²	The mean basal area of each mature tree during initial sampling	Live mature aspen Live mature conifers
Standard deviation of individual basal area	m ²	The standard deviation of each mature trees’ basal area, during initial sampling	Live mature non-aspen hardwoods [†]
Initial quadratic mean diameter	cm	Quadratic mean diameter of mature trees present in plot during initial sampling	Live mature non-aspen trees
Initial suckers plus juveniles	Unitless	Number of aspen suckers plus juveniles present in subplots during initial sampling	Live aspen stems < 5.1 cm DBH
Final seedling plus juvenile sum	Unitless	Number of seedlings plus juveniles present in subplots during final sampling	Live conifers < 5.1 cm DBH Live non-aspen hardwoods [†] < 5.1 cm DBH Live non-aspen trees < 5.1 cm DBH
Relative aspen abundance by count	Unitless	The ratio of the number of live mature aspen to the total number of live mature trees, during the initial sampling	NA
Relative aspen abundance by basal area	Unitless	The ratio of mature aspen live basal area to total stand mature tree live basal area, during the initial sampling	NA

[†] Hardwood species include *Acer grandidentatum*, *Alnus* spp., *Populus trichocarpa*, and *Salix* spp.

Table 4. Table 4. Best performing generalized linear model for each response variable. Models (a) and (b) use a gaussian error distribution and an identity link function. Models (c)-(f) use a negative binomial error distribution and a log link function. Mature stem recruitment counts (c) are offset by number of years of the study period and number of mature aspen stems in the initial sampling. Model fit statistics are R² values for gaussian models and McFadden's pseudo R² values for negative binomial models. Relative importance refers to cumulative AIC weight of all candidate model containing each predictor, normalized from zero to one.

Response	Predictor	Standardized estimate	Estimate (\pm SE)	p	Relative importance	df	Model fit statistic
a. Mortality rate	Intercept	4.2495	4.2495 (0.1608)	<0.001		177	0.390
	Mean initial canopy dieback rating	1.3979	3.0314 (0.3631)	<0.001	1.00		
	Annual VPD deviation	-0.6354	-1.5739 (0.5463)	0.004	0.76		
	Annual temperature range	0.5839	0.2042 (0.0639)	0.002	0.71		
	Initial total dead basal area	0.5254	0.0792 (0.0269)	0.004	0.59		
	Potential incident solar radiation	-0.4096	-5.0431 (2.2661)	0.027	0.86		
	Annual precipitation deviation	-0.4019	-3.5395 (1.8029)	0.051	0.61		
b. Growth rate (log transformed)	Intercept	0.6080	0.6080 (0.0494)	<0.001		150	0.265
	Initial total live basal area	-0.2730	-0.0092 (0.0020)	<0.001	1.00		
	Mean summer vapor pressure	0.1386	1.2891 (0.5195)	0.014	0.66		
	Mean annual high temperature	0.1381	0.0812 (0.0317)	0.012	0.18		
	Std dev of individual aspen basal area	0.1045	5.1615 (2.8842)	0.076	0.71		
	Topographic position index 100m radius	-0.0842	-0.0235 (0.0153)	0.125	0.68		
c. Recruitment to mature stem size class	Intercept	-4.5687	-4.5687 (0.1286)	<0.001		179	0.103
	Initial aspen live basal area	-0.5192	-0.0316 (0.0087)	<0.001	0.86		
	Mean spring SWE	-0.4150	-0.0040 (0.0016)	0.015	0.35		
	Mean annual PDSI	0.2693	0.5161 (0.3199)	0.107	0.18		
d. Sapling count	Intercept	0.5821	0.5821 (0.0979)	<0.001		177	0.276
	Mean Summer CWD	0.4738	0.0059 (0.0012)	<0.001	0.99		
	Initial aspen suckers plus juveniles	0.4095	0.0106 (0.0023)	<0.001	1.00		
	Initial total live basal area	-0.3654	-0.0153 (0.0057)	0.007	0.99		
	Initial total live basal area x Mean summer CWD	0.3449	0.0002 (0.0001)	0.004	0.95		
	Initial total adult tree count	-0.3007	-0.0388 (0.0165)	0.018	0.88		
e. Juvenile count	Intercept	2.1330	2.1330 (0.1135)	<0.001		143	0.075
	Elevation	0.6297	0.0016 (0.0004)	<0.001	0.76		
	Summer CWD deviation	0.4791	1.8442 (0.5612)	0.001	0.67		
	Winter high temperature deviation	0.1942	0.9430 (0.5734)	0.100	0.57		
f. Sucker count	Intercept	1.7886	1.7886 (0.1265)	<0.001		142	0.330
	Stream presence	1.0557	1.0557 (0.4034)	0.009	0.97		
	Mean winter VPD	0.7383	10.9739 (2.0818)	<0.001	0.96		
	Seasonality of precipitation	0.3044	0.0167 (0.0070)	0.018	0.42		

Table S1. Main effect and interaction terms included in candidate linear models for each aspen response. Relative importance refers to cumulative AIC or AIC_C weight of all candidate models containing each predictor, normalized from zero to one. Terms included in final model for each response variable are indicated by bold typeface.

Response variable	Model term	Relative importance
Annual percent mortality	Mean initial canopy dieback rating	1.00
	Potential incident solar radiation	0.86
	Deviation in annual VPD	0.76
	Annual temperature range	0.71
	Deviation in annual precipitation	0.61
	Initial total tree count	0.60
	Initial total dead basal area	0.59
	Initial aspen dead basal area	0.38
	Diurnal temperature range	0.30
	Deviation in fall high temperature	0.21
	Deviation in annual SWE	0.20
	Deviation in fall VPD	0.17
	Longitude	0.14
	Initial aspen tree count	0.13
	SWE mean annual difference from normal	0.08
	Initial total tree count x Deviation in annual VPD	0.24
	Potential incident solar radiation x Deviation in annual VPD	0.20
	Initial total tree count x Potential incident solar radiation	0.13
Potential incident solar radiation x Deviation in annual precipitation	0.12	
Initial total tree count x Deviation in annual precipitation	0.06	
Annual percent recruitment of mature stems	Initial aspen live basal area	0.86
	Mean spring SWE	0.35
	Deviation in summer CWD	0.24
	Mean annual SWE	0.22
	Elevation	0.22
	Mean annual PDSI	0.18
	Minimum winter PDSI	0.17
	Deviation in spring PDSI	0.17
	Mean spring high temperature	0.14
	Deviation in winter vapor pressure	0.12
	Deviation in fall high temperature	0.09
	Mean fall high temperature	0.07
	Mean annual high temperature	0.06
	Mean winter PDSI	0.05
	Mean summer high temperature	0.05
	Initial aspen live basal area x Mean spring SWE	0.09
Elevation x Mean spring SWE	0.05	
Initial aspen live basal area x Mean annual high temperature	0.01	
Growth rate	Initial total live basal area	1.00
	Standard deviation of individual aspen basal area	0.71
	Topographic position index (100 m radius)	0.68
	Mean summer vapor pressure	0.66
	Deviation in fall precipitation	0.35

	Mean spring high temperature Latitude Mean annual high temperature Mean summer high temperature Maximum summer high temperature Mean winter high temperature Mean fall high temperature Seasonality of temperature Minimum annual PDSI Deviation in fall high temperature Initial stand basal area x Topographic position index (100 m radius) Deviation in fall precipitation x Topographic position index (100 m radius) Initial stand basal area x Deviation in fall high temperature Mean spring high temperature x Topographic position index (100 m radius)	0.30 0.25 0.18 0.18 0.16 0.16 0.14 0.12 0.09 0.09 0.23 0.15 0.09 0.07
Sapling density	Initial aspen suckers plus juveniles Mean summer CWD Initial total live basal area Initial total tree count Seasonality of temperature Deviation in summer vapor pressure Mean annual CWD Mean spring VPD Mean annual VPD Mean fall CWD Mean summer VPD Mean summer PDSI Mean fall PDSI Deviation in summer PDSI Mean annual PDSI Initial total live basal area x Mean summer CWD Mean summer CWD x Initial aspen sucker plus juvenile sum Initial total tree count x Mean summer CWD	1.00 0.99 0.99 0.88 0.32 0.29 0.00 0.00 0.00 0.00 0.00 0.00 0.00 0.00 0.00 0.00 0.95 0.33 0.26
Juvenile density	Elevation Deviation in summer CWD Deviation in winter high temperature Standard deviation of individual aspen basal area Longitude Deviation in fall precipitation Initial aspen quadratic mean diameter Vapor pressure mean annual difference from normal Deviation in fall CWD High temperature mean annual difference from normal Deviation in summer high temperature Seasonality of temperature Deviation in summer precipitation Deviation in fall vapor pressure Deviation in annual high temperature Elevation x Deviation in summer CWD Elevation x Deviation in winter high temperature Standard deviation of individual aspen basal area x Deviation in summer	0.76 0.67 0.57 0.44 0.29 0.29 0.20 0.12 0.11 0.10 0.09 0.09 0.06 0.04 0.03 0.26 0.13 0.10

	CWD Standard deviation of individual aspen basal area x Deviation in winter high temperature	0.07
Sucker density	Stream presence Mean winter VPD Seasonality of precipitation Deviation in fall vapor pressure Deviation in winter high temperature High temperature mean annual difference from normal CWD mean annual difference from normal Deviation in fall CWD Deviation in annual CWD Deviation in annual VPD Mean summer CWD Mean fall VPD Mean fall CWD Deviation in fall precipitation Mean annual CWD Stream presence x High temperature mean annual difference from normal Stream presence x Deviation in annual CWD Stream presence x Deviation in fall precipitation	0.97 0.96 0.42 0.33 0.28 0.28 0.23 0.19 0.14 0.09 0.09 0.02 0.01 0.00 0.00 0.07 0.04 0.00